NASA TECHNICAL HANDBOOK

NASA-HDBK-4006

National Aeronautics and Space Administration
Washington, DC 20546-0001

Approved: 06-03-2007
Superseding NASA-STD-(I)-4005

LOW EARTH ORBIT SPACECRAFT CHARGING DESIGN HANDBOOK

MEASUREMENT SYSTEM IDENTIFICATION:
METRIC

DOCUMENT HISTORY LOG

Status	Document Revision	Approval Date	Description
Baseline		06-03-2007	Baseline Release Interim Standard NASA-STD-(I)-4005 was transitioned to this handbook and the standard, NASA-STD-4005. Made editorial and formatting changes. Replaced figure 10 with new figure 10 which includes “ISS Capacitance” in the legends definition area.

FOREWORD

This handbook is published by the National Aeronautics and Space Administration (NASA) as a guidance document that provides engineering information; lessons learned; possible options to address technical issues; classification of similar items, materials or processes; interpretative direction and techniques; and any other type of guidance information that may help the Government or its contractors in the design, construction, selection, management, support, or operation of systems, products, processes, or services.

This handbook is approved for use by NASA Headquarters and NASA Centers, including Component Facilities.

This handbook provides design guidance for high-voltage space power systems (>55 volts) that must operate in the plasma environment associated with Low Earth Orbit (LEO).

Requests for information, corrections, or additions to this handbook should be submitted via "Feedback" in the NASA Technical Standards System at http://standards.nasa.gov.

Original Signed By

Christopher J. Scolese	06-03-2007
NASA Chief Engineer	Approval Date

TABLE OF CONTENTS

SECTION **PAGE**

LIST OF FIGURES

LIST OF TABLES

Low Earth Orbit Spacecraft Charging Design Handbook

1. SCOPE

The information in this handbook presents an overview of the current understanding of the various plasma interactions that can result when a high-voltage system is operated in the Earth's ionosphere, references common design practices that have exacerbated plasma interactions in the past, and recommends standard practices to eliminate or mitigate such reactions.

1.1 Purpose

The purpose of this handbook is to provide design guidance referenced in NASA-STD-4005, *Low Earth Orbit Spacecraft Charging Design Standard,* for high-voltage space power systems (>55 volts) that operate in the plasma environment associated with LEO (altitude from 200 and 1000 km and latitude between -50 and +50 degrees). Such power systems, particularly solar arrays, are the proximate cause of spacecraft charging in LEO, and these systems can interact with this environment in a number of ways that are potentially destructive to themselves as well as to the platform or vehicle that has deployed them.

1.2 Applicability

This handbook is applicable to high-voltage space power systems that operate in the plasma environment associated with LEO (see NASA-STD-4005).

This handbook may be referenced in contract, program, and other Agency documents for guidance.

2. APPLICABLE DOCUMENTS

2.1 General

The documents listed in this section are applicable to the guidance in this handbook. The latest issuances of cited documents apply unless otherwise specified. The applicable documents are accessible via the NASA Technical Standards System at http://standards.nasa.gov, directly from the Standards Developing Organizations, or from other document distributors.

2.2 Governmen t Documents

NASA-STD-4005	Low Earth Orbit Spacecraft Charging Design Standard

2.3 Non-Government Documents

AFWAL-TR- 88-4143, Volume 2	Design Guide: Designing and Building High Voltage Power Supplies, Materials Laboratory

2.4 Order of Precedence

When this handbook is referenced in a contract or in program or project documentation, the technical requirements of the document referencing this handbook take precedence, in case of conflict, over guidance cited in applicable documents or referenced guidance documents.

3. ACRONYMS AND DEFINITIONS

3.1 Acronyms

AC	Alternating Current
AFWAL	Air Force Wright Aeronautical Laboratories
AMU	Atomic Mass Unit
APSA	Advanced Photovoltaic Solar Array
CHAWS	Charging Hazards and Wake Studies
DC	Direct Current
EMI	Electromagnetic Interference
EMU	Extra-vehicular Maneuvering Unit (spacesuit)
EOS-AM1	Earth Observing System – Morningside 1 (now Terra)
ESA	European Space Agency
EURECA	European Retrievable Carrier
EUV	Extreme Ultraviolet
EVA	Extra-vehicular Activity (spacewalk)
EWB	Environmental WorkBench
FEF	Field Enhancement Factor
FPP	Floating Potential Probe
GEO	Geosynchronous Earth Orbit
GRC	Glenn Research Center
IRI	International Reference Ionosphere
ISS	International Space Station
ITAR	International Traffic-in-Arms Regulations
JAXA	Japanese Space Agency
LEO	Low Earth Orbit (200-1000 km altitude, -50 to +50 latitude, for the purposes of this document)
LeRC	Lewis Research Center (now GRC)
MET	Marshall Engineering Thermosphere
MSFC	Marshall Space Flight Center
MSIS	Mass Spectrometer Incoherent Scatter
NASA	National Aeronautics and Space Administration
NASCAP	NASA Charging Analyzer Program
NASCAP-2K	NASA/Air Force Spacecraft Charging Analyzer Program
PAS-6	Space Systems/Loral Commercial Communications Satellite

PASP Plus	Photovoltaic Array Space Power Plus Diagnostics
PC	Personal Computer
PCU	Plasma Contactor Unit
PIX-II	Plasma Interactions Experiment - II
PMAD	Power Management and Distribution
PMG	Plasma Motor Generator
ProSEDS	Propulsive Small Expendable Deployer System
RCS	Reaction Control System (attitude thrusters)
RTV	Room Temperature Vulcanized-rubber
SAIC	Science Applications International Corporation
SAMPIE	Solar Array Module Plasma Interactions Experiment
SPENVIS	Space Environment Information System
TSS-1R	Tethered Satellite System – first reflight
UV	Ultraviolet

3.2 Definitions

The following definitions are based on AFWAL-TR-88-4143, Volume 2, *Design Guide: Designing and Building High Voltage Power Supplies, Materials Laboratory*:

Breakdown Voltage: The voltage at which the insulation between two conductors fails.

Capacitance (Capacity): That property of a system of conductors and dielectrics that permits the storage of electricity when potential difference exists between the conductors. The ratio of the charge on one of the conductors of a capacitor to the potential difference between the conductors. (There will be an equal and opposite charge on the other conductor.)

Capacitor (Condenser): A device whose primary purpose is to introduce capacitance into an electric circuit.

Cathode: The electrode through which an electric current leaves a liquid, gas, or other discrete part of an electric circuit; the negatively charged pole of an electrochemical cell.

Cell: A single unit capable of serving as a direct current (DC) voltage source by transfer of ions in the course of a chemical reaction.

Charge: In electrostatics, the amount of electricity present upon any substance that has accumulated electric energy.

Conductance: The reciprocal of resistance. The ratio of current passing through a material to the potential difference at its ends.

Conductivity: Reciprocal of resistivity.

Conductor: An electrical path that offers comparatively little resistance. A wire or combination of wires not insulated from each other, suitable for carrying a single electric current.

Contaminant: An impurity or foreign substance present in or on a material and affecting one or more properties of the material.

Corona: A non-self-sustaining discharge (sometimes visible) due to ionization of the gas surrounding a conductor around which exists a voltage gradient exceeding a certain critical value for a gaseous medium.

Dielectric: A non-conducting material.

Dielectric Breakdown: An electrical discharge within a dielectric due to an applied electric field in excess of the dielectric strength of the material.

Dielectric Constant (relative permittivity): Property of a dielectric that determines the electrostatic energy stored per unit volume for unit potential gradient.

Dielectric Strength: The maximum electrical potential gradient (electric field) that an insulating material can withstand without rupture, usually expressed in volts per mm of thickness.

Electric Field Intensity: The force exerted on a stationary positive charge per unit charge at a point in an electric field. Designated by E. Also known as electric field strength, electric field vector. For a point charge in space, it is given by

$$E = \frac{Q}{4\pi\varepsilon r^2}$$

where r is the distance from the charge Q and ε is dielectric constant.

Electrode: A conductor, not necessarily metal, through which a current enters or leaves an electrolytic cell, arc, furnace, vacuum tube, gaseous discharge tube, or any conductor of the nonmetallic class.

Electron: A stable elementary, negatively charged particle that circles around the center or nucleus in an atom.

Electrostatic Discharge: A sudden and large increase in current through an insulation medium due to the complete failure of the medium under the electrostatic stress.

Encapsulating: Enclosing an article in an envelope of plastic or other sealant.

Flashover: A disruptive electrical discharge around or over the surface of a solid or liquid insulator.

Floating Potential: The potential a spacecraft comes to under current balance with the surrounding plasma.

Frequency: The number of complete cycles or vibrations per unit of time.

Gradient: Rate of increase or decrease of a variable parameter.

Hollow Cathode: An efficient plasma-emitting device flowing gas through a hollow orifice.

Impedance: The total opposition that a circuit offers to the flow of alternating current (AC) or any other time varying current at a particular frequency. It is a combination of resistance R and reactance X, measured in ohms, and designated by $Z=(R^2 + X^2)^{1/2}$.

Impulse: A unidirectional surge generated by the release of electric energy into an impedance network.

Insulation: Material having a high resistance to the flow of electric current to prevent leakage of current from a conductor.

Insulation Resistance: The ratio of the applied voltage to the total current between two electrodes in contact with a specific insulator.

Insulation System: All of the materials used to insulate a particular electrical or electronic product.

Insulator: A material of such low electrical conductivity that the flow of current through it can usually be neglected.

Ion: An electrified portion of matter of sub-atomic, atomic, or molecular dimensions such as is formed when a molecule of gas loses an electron (when the gas is stressed electrically beyond the critical voltage) or when a neutral atom or group of atoms in a fluid loses or gains one or more electrons.

Ionization: Generally the dissociation of an atom or molecule into positive or negative ions or electrons. Restrictively, the state of an insulator whereby it facilitates the passage of current due to the presence of charged particles (usually induced artificially).

Particulate (space particulate debris): The sources of spacecraft particulate debris are Earth, spacecraft, and space environments. Earth particulate is mostly dust, sand, and rocket exhaust. Sources are materials spalled by cosmic dust impacts on materials and the solar array, outgassing products, and slip rings. Space environment consists of residues that form the space plasma, cosmic dust of masses less than one gram, micrometeoroids, and meteoroids.

Paschen Discharge: Breakdown of neutral gas in a high electric field.

Permittivity: The dielectric constant multiplied by the permittivity of empty space, where the permittivity of empty space, ε_0, is a constant appearing in Coulomb's Law.

Plasma: A gaseous body of ions and electrons of sufficiently low density that considerable charge separation is possible. Because of the mobility of charge, a plasma is normally neutral and free of electric field in its interior, just like a metallic conductor.

Plasma Arcing: Electrical discharges which are a consequence of the presence of a plasma at the site of the discharge.

Plasma Ground: See Plasma Potential.

Plasma Potential: The potential which accelerates neither electrons nor positively charged ions toward a surface.

Plasma Temperature: The kinetic temperature of a thermal plasma. Often this is expressed in energy units (eV), giving the average thermal energy of an ion or electron in the plasma. The ion temperatures need not be the same as the electron temperature in a plasma.

Plastic: High polymeric substances, including both natural and synthetic products, but excluding the rubbers, that are capable of flowing under heat and pressure at one time or another.

Polyimide: A polymer often used for spacecraft thermal control because of its yellow color. Very thermally stable, this polymer is often also used for flexible solar array blankets. Kapton® is a polyimide.

Polymer: A compound formed by polymerization that results in the chemical union of monomers or the continued reaction between lower molecular weight polymers.

Polymerize: To unite chemically two or more monomers or polymers of the same kind to form a molecule with higher molecular weight.

Potential: The work per unit charge required to bring any charge to the point from an infinite distance.

Power: The time rate at which work is done. Power is obtained in watts if work is expressed in joules and time is in seconds.

Pressure: Force per unit area. Absolute pressure is measured with respect to zero pressure. Gauge pressure is measured with respect to atmospheric pressure.

Primary Arc: Trigger arc. An initial electrical discharge that may or may not trigger another type of discharge.

Pulse: A wave that departs from a first nominal state, attains a second nominal state, and ultimately returns to the first nominal state.

RC Time Constant: Time constant obtained by multiplying resistance by capacitance.

Resistance: Property of a conductor that determines the current produced by a given difference of potential. The ohm is the practical unit of resistance.

Resistivity (specific insulation resistance): The electrical resistance between opposite faces of a 1-cm cube of an insulating material, commonly expressed in ohm-centimeters. Sometimes called volume resistivity.

Semiconductor: A solid crystalline material whose electrical conductivity is intermediate between that of insulators and conductors, and is usually applied field and temperature dependent.

Sizzle Arc: A sustained electric discharge due to dielectric breakdown.

Snapover: The phenomenon caused by secondary electron emission that can lead to electron collection on insulating surfaces in an electric field.

Solar Array: Solar cells connected in series and/or parallel to generate power. Often the sole power source for a spacecraft.

Solar Cell: A photovoltaic device used to convert the energy in light to electrical energy.

String Voltage: The voltage of a single series-connected solar array segment. Often this is the power system voltage.

Surface Creepage Voltage: See Creepage.

Surface Flashover: See Flashover.

Surge: A transient variation in the current and/or potential at a point in the circuit.

Sustained Arc: An electrical discharge that lasts much longer than the usual capacitance-discharging arc (on the order of 1 millisecond or longer).

Transient: That part of the change in a variable that disappears during transition from one steady state operating condition to another.

Voltage: The term most often used in place of electromotive force, potential difference, or voltage drop to designate electric pressure that exists between two points and is capable of producing a flow of current when a closed circuit is connected between the two points.

Wire: A metallic conductor of round, square, or rectangular cross-section that can be either bare or insulated.

4. GUIDANCE

4.1 Reference Documents

An important reference document for LEO spacecraft charging design is Ferguson and Hillard, 2003. It contains an extensive annotated bibliography that is not possible to repeat here. A good (and current) reference for test procedures is Ferguson et al., 2005. The handbook information, based largely on Ferguson and Hillard, 2003, is contained in appendices A through F. For other documents referenced in the appendices, see appendix G.

APPENDIX A
OVERVIEW OF PLASMA INTERACTIONS

A.1 Poisson Equation

When energized conductors are exposed to plasma, positive surfaces collect electrons and negative surfaces collect ions. The Poisson equation governs potential distributions which determine charge movement. The Poisson Equation is

$$\nabla^2\varphi = -4\pi\rho, \qquad \text{(eqn. A.1.1)}$$

where φ is the potential, and ρ is the charge density. When the charge density is very low, as in Geosynchronous Earth Orbit (GEO), Poisson's equation reduces to Laplace's equation.

Electrons, which are much lighter and more mobile than ions, are collected more easily. Surfaces, therefore, charge to whatever potential necessary for the net current flow to be zero in equilibrium. A current loop forms that uses the ionosphere as part of the conducting path. The potential that any given surface will achieve is very difficult to model and generally requires full-up testing in a plasma environment. The resulting interactions can be summarized as follows:

a. Surfaces that are more negative than ≈ 100 V with respect to their surroundings are subject to arcing. These arcs can be either plasma arcs or arcs to adjacent conductors. They are usually a momentary discharge of accumulated energy, lasting only milliseconds, but under some conditions can be sustained. The necessary conditions for the arc to be sustained are for the current and voltage to be maintained above threshold values. Plasma arc thresholds are poorly known but can be as low as -50 V under some conditions.

b. Surfaces that are more negative than ≈ 100 V are subject to ion bombardment and sputtering. Since the dominant ion is atomic oxygen, care must be taken that chemical attack does not occur as well.

c. Surfaces that are positive can easily collect sufficient electrons to present a measurable power drain to the system. Referred to as "parasitic current collection," this condition can result in a few percent power loss to the system.

d. If the power system is negatively grounded, as is most commonly done, the entire vehicle can float negative with respect to the ionosphere. The system potential can become as negative with respect to the ionosphere as the entire power system voltage. For systems with very large areas of high-voltage surfaces, such as the International Space Station (ISS), this effect is large, requiring a plasma contactor to mitigate it. Note that when ISS has its plasma contactor (grounded to the structure) operating, current collection from the plasma of the solar arrays is exacerbated, because the arrays will be held at positive potentials with respect to the surrounding plasma.

APPENDIX B
ENVIRONMENTS

B.1 The Ambient Environment

B.1.1 The Neutral Atmosphere

The dominant environment between 100 and 1000 km is the neutral atmosphere. In this essentially collision-less regime, the gases are in hydrostatic equilibrium. Below about 100 km, where the atmosphere is homogeneous, the composition is approximately 80 percent N_2 and 18 percent O_2 with traces of NO_2, Ar, and other gases. Above 100 km, atomic oxygen, the result of photo-dissociation of molecular oxygen comes to dominate. Above about 800 km the atmosphere is largely atomic hydrogen. At a 500 km altitude, the neutral number density varies from $2x10^6$ to $3x10^8$ cm^{-3}, depending on solar activity and position in the orbit. The kinetic temperature of the gas is usually between 500 and 2000 K, and the ambient pressure is in the range of 10^{-10} to $5x10^{-8}$ Torr.

The neutral gas environment has been well explored and quantified. Empirical models based on in-situ neutral composition and satellite drag measurements have evolved over the years into reliable predictors of the average composition and thermal structure of the thermosphere. The most notable of these models are the Mass Spectrometer Incoherent Scatter (MSIS-86) model (Hedin, 1987; Prag, 1983) based on in-situ satellite observations of neutral concentrations, the Marshall Space Flight Center (MSFC) version of the Jacchia model derived from satellite drag measurements, the Marshall Engineering Thermosphere (MET) ("Computational procedure," 1970; Hickey, 1988) and the U.S. Standard Atmosphere ("U.S. standard," 1976; King, 1978). These models provide good estimates of the thermosphere environment as functions of altitude, longitude, latitude, local time, magnetic activity, and solar activity and are continually updated as new information becomes available.

B.1.2 The Plasma Environment

On the sunlit hemisphere of the Earth, ultraviolet (UV) and extreme-ultraviolet (EUV) radiation penetrates the atmosphere, ionizing and exciting the molecules present. This results in a fine balance between increasing density and increasing absorption that leads to the formation of layers, the ionosphere. A highly dynamic plasma, the ionosphere's properties vary with altitude, latitude, time of day, and sunspot cycle. Over hours to weeks, local geomagnetic disturbances can cause dramatic variations that are difficult to predict. Despite these complications, the broad features of the ionosphere can be described with simple models.

The variability with latitude, known since the 1920s, is so dramatic that the ionosphere is conventionally divided into three distinct regions: high-latitude, mid-latitude, and low-latitude. The easiest region to understand is the mid-latitude region, which most closely follows classical ionospheric models. In this document, spacecraft design is not treated for the high-latitude region.

Variation with altitude is perhaps the most important parameter for the spacecraft designer. This pronounced vertical structure is not simply a matter of height variation but reflects basic physical

processes that differ in the resulting regions. Three processes, in particular, are responsible: (1) the sun's energy is deposited at various heights because of the absorption characteristics of the atmosphere, (2) the physics of recombination depends on density and therefore on altitude, and (3) composition of the atmosphere changes with height.

The lower limit of the ionosphere is somewhat arbitrary since plasma production falls off continuously with decreasing height. Historically, the ionosphere has been assumed to begin about 50 km from the surface, because this is the altitude where plasma density becomes sufficient to affect radio wave propagation noticeably. There is no distinct upper limit, but 2000 km is generally used for most practical applications. In this document, spacecraft design for altitudes above 1000 km is not specified, because of the radiation issues that are a primary design driver.

Four layers describe the vertical structure of the ionosphere. In order of increasing altitude and increasing plasma density, these are designated as D, E, F1, and F2 regions. Their properties are summarized in table 1.

Table 1—Nominal Properties of Ionospheric Layers

Region	Nominal Height of Peak (km)	Plasma Density at Noon (cm^{-3})	Plasma Density at Midnight (cm^{-3})	Dominant Ion
D	90	~1.5×10^4	vanishes	O_2^-
E	110	~1.5×10^5	~1×10^4	O_2^+
F1	200	~2.5×10^5	vanishes	O^+
F2	300	~1.0×10^6	~1.0×10^5	O^+

Beyond the peak in the F2 layer, electron density decreases monotonically out to several Earth-radii. For altitudes up to and including the F2 peak, thermal energies of the electrons and ions are in the range of 0.1 to 0.2 eV, corresponding to kinetic temperatures of 1200 to 2400 K. Temperature rises monotonically beyond this point, reaching several thousand eV in geosynchronous orbits.

The F2 layer is the most important for spacecraft operations. It is in this layer that ISS lives, the Shuttle orbiter and most LEO spacecraft fly, and the Hubble telescope orbits to photograph the universe. Its boundaries and electron density are highly variable, with a general erratic behavior imposed on large daily, seasonal, and solar cycle variations.

Ionospheric plasma distributions within the F-region have been extensively explored since the advent of bottom-side sounders, long before in-situ satellite observations were made. As a result, the general morphology of the F-region and some of its more prominent individual features are well understood. While there are detailed features such as localized troughs, localized heating, and short temporal variations that are difficult to model, the overall global

structure of the ionosphere is now well understood, and excellent ionospheric models exist for estimating and quantifying plasma distributions. In particular, the global International Reference Ionosphere model (IRI-90, for example) provides estimates under varying solar activity conditions of plasma concentrations, composition, and temperatures as a function of altitude, time, and location. Another good reference is BSR/AIAA G-003B-2004, American National Standard, *Guide to Reference and Standard Atmosphere Models.*

B.2 The Spacecraft-Induced Environment

Spacecraft-induced environments can take many forms: neutral gases, ionized gases (plasmas), condensable gases, particulates, radiation, etc. In many cases, these environments can overwhelm the natural environment and can lead to undesirable interactions. Below, these types of environments are treated separately.

Cold gas thrusters and Reaction Control System (attitude thrusters) (RCS) can significantly increase the localized neutral pressure. This increase can be dangerous when there are exposed high-voltage conductors, because Paschen discharges can occur (see appendix D, section D.2.3). In general, if the local neutral pressure is more than a milliTorr and less than a few Torr, high-voltage electrical breakdowns can occur. At a voltage of -3500 V relative to the Orbiter, the Tethered Satellite System – first reflight (TSS-1R) tether leaked gas into its deployer control reel enclosures and the elevated neutral pressure led to Paschen discharge and loss of the mission (Szalai et al., 1996). On the Solar Array Module Plasma Interactions Experiment (SAMPIE, Ferguson and Hillard, 1997) Shuttle payload bay experiment, a local gas vent had to be moved to prevent Paschen discharge. Helium is the most dangerous neutral effluent gas, since it has the lowest Paschen breakdown minimum voltage.

Ionized gases can be emitted by plasma sources such as hollow cathode plasma contactors or from neutral gas sources at high positive potentials. Locally, the plasma density can be greater than the ambient plasma density, and similar plasma interactions can occur with high-voltage components. On ISS, the plasma contacting units (PCUs), when operating, produce a local xenon plasma of much greater density than ambient. It has been estimated that the invisible plasma ball produced is some eight meters in radius before its density decreases below the ambient plasma density in LEO. Arcing and current collection from such a plasma could occur in much the same way as with an ambient plasma, implying that solar arrays and other active sites should be kept out of induced plasma plumes.

Condensable gases are effluents that can condense on cold components and contaminate their surfaces. Oil and water vapor are two major condensables that can influence the interactions of spacecraft surfaces. In vacuum chamber testing, oil has been shown to prevent snapover on surfaces when high positive voltages are used (see section C.1.1.4.3 below). Many oils, however, cannot withstand the LEO atomic oxygen environment on ram-facing surfaces but can build up on wake surfaces. Water vapor released on the night side can condense on insulating surfaces of solar arrays, etc., and can participate in arcing when the arrays become active in sunlight. It has been shown in laboratory testing that solar arrays that have been thoroughly baked out (heated in a vacuum for seven days) lose the water vapor contamination that is important in low-voltage (-100 to -300 V) arcing (Vayner et al., 2002). In LEO, however, a cold cycle is about 1/3 of every orbit. Even very well baked-out systems can have recondensation

from effluents evolved during the night side of the orbit. Thin layers of condensed contaminants can concentrate electric fields above high-voltage conductors, even to the point where they undergo dielectric breakdown.

Particulates can be emitted or shaken from surfaces, but can also result from arcing or sputtering from spacecraft surfaces. Particulates can transfer small amounts of charge from one surface to another, but their major effect is in changing the characteristics of the surfaces to which they adhere. For instance, an insulating particle on a conductor that is at a high potential can concentrate the electric field structure locally, possibly leading to a reduced arcing voltage threshold.

Radiation can embed electrons deep within dielectrics where they can build up for days, weeks, or months until the dielectric breaks down under the induced electric field. In the natural environment, this effect will mainly happen in the auroral zones, radiation belts, and above the South Atlantic Anomaly, and thus are not usually important in the environment for which this handbook is applicable; but radiation produced on or within a spacecraft can be important regardless of orbital position. Satellites using radioactive power sources must be designed to ameliorate this “deep-dielectric” charging, which is different from the typical “surface” spacecraft charging.

APPENDIX C
PLASMA INTERACTIONS

C.1 Exposed High-Voltage Conductors

It is almost always unwise to allow exposed high-voltage (|V| > 55 V) conductors on spacecraft. Exposed high-voltage conductors that do not exhibit corona or Paschen breakdown in a neutral gas can readily do so if the environment contains a significant ionized component. Although a high-voltage surface—solar cell interconnects, for example—can be exposed to the ionized space plasma by design, surfaces can also be at high voltages because of current collection from the plasma. The resulting equilibrium potentials that are assumed by surfaces result in the following effects and are described in the sections that follow:

a. Floating potential shifts: In equilibrium, some parts of the spacecraft can be charged to negative voltages near the maximum string voltage of the solar array.

b. Parasitic power drain: Direct loss of power due to current collection. This loss can be several percent of total power.

c. Sputtering: Surfaces that charge negative will attract ions that in turn will result in sputtering of the material.

d. Arcing: Negative surfaces undergo arcing when some critical threshold is exceeded.

C.1.1 Current Collection

C.1.1.1 The Current-Balance Condition

In the weakly ionized low-density plasma found in LEO, current collection is completely described by Poisson's equation (eqn. A.1.1). Positive surfaces readily attract electrons and negative surfaces attract the much more massive positive ions only with great difficulty. Since in equilibrium, net current collection must be zero, surfaces will charge to equalize the net current of each polarity.

To illustrate the basic effects, consider first a hypothetical experiment. Suppose two metal spheres a few feet in diameter are initially connected by a conductor and placed in LEO some distance apart. Since electrons are collected more easily than ions, both spheres will charge to the same potential, within a volt or two of plasma potential. Now suppose a high-voltage battery is placed between them with one sphere connected to the negative terminal and the other to the positive. On Earth, in air, such an arrangement would result in half of the battery voltage appearing on each sphere. But in LEO, highly mobile electrons stream to the positive sphere while the negative sphere struggles to collect the massive ions. Both experience and modeling indicate that approximately 90 percent of the battery voltage will appear on the negative sphere and only 10 percent will be on the positive one with respect to the plasma potential.

The implications of this phenomenon are considerable and often expensive. In the case of ISS, for example, the power system consists of solar arrays wired in a series-parallel arrangement to

give a 160-volt system. Since the main structure of ISS is "grounded" to the negative end of the array string, the entire Space Station would "float" more than 140 V negative with respect to the ionosphere. Such potentials are beyond the dielectric strength of the anodized coatings on the ISS aluminum structure, and would lead to arcing into the space plasma and eventual destruction of the ISS thermal control system. This prospect required the addition of an active plasma contactor, a xenon hollow cathode discharge unit, to effectively ground the Space Station to the ionosphere. As it turns out, the ISS solar arrays are unusual in that they are poor electron collectors because of their welded-through design. Atypically, the ISS early mission-build structure usually does not charge more than 20 volts or so negative with respect to the surrounding plasma even without the plasma contactors operating. However, as more solar arrays are put up, it is expected that the charging level on ISS will increase dramatically, justifying the added expense of the plasma contactors (Ferguson and Gardner, 2002).

For conducting surfaces that are covered with insulators, some elapsed time could be necessary for the steady state potential situation to be reached. The surfaces will charge until no further charge collection is necessary in equilibrium, and this is tantamount to charging up a capacitor with plate separation equal to the insulator thickness. Ion charging times in LEO can be considerable for typical anodized aluminum thicknesses. It is estimated, for instance, that in the daytime ionosphere, ISS surfaces will take 4 seconds to fully charge, whereas on the morning terminator where the ionospheric ion density is at its lowest, charging times of 40 seconds or more can occur.

C.1.1.2 Sheath Effects

A positively charged spherical electrode will collect electrons when inserted in a plasma. The volume called the "sheath," in which the electrode influences electrons, is larger than the sphere. For low voltages, the sheath thickness will be nearly the same as the Debye length (see equation in appendix D, section D.2.3.1). Some electrons will orbit around the electrode and escape from the sheath. The collected or trapped electrons are said to be orbit-limited and are affected in a complex manner by the radius of the electrode, the electrode voltages, and the temperature and density of the free electrons.

A solar array looks to the plasma like a large rod electrode (like the wires and interconnects that are in contact with the plasma) rather than a spherical probe, and is also surrounded by a sheath. Power loss caused by plasma leakage current will become significant above 100 V for positive electrodes (see section following). Above a threshold voltage, which differs because of array design, arcing can be observed between the electrodes.

C.1.1.3 Current Collection by Structures

C.1.1.3.1 Electron Collection

LEO spacecraft are traveling subsonically with respect to the electrons in the ambient plasma. That is, at the plasma temperatures in LEO, the ambient electrons are moving at speeds greatly in excess of the orbital velocity. Thus, electrons can be collected on any conducting surface (exposed to the undisturbed plasma, i.e., not in the plasma wake) that is not charged more than a few electron temperatures negative. In general, electron collection is well described by probe

theory. See for example Chen, 1965. For large surfaces, collection is best described by thin sheath probe theory. For structures smaller than a few times the Debye length (see equation in appendix D, section D.2.3.1), orbit-limited theory can be used. Electron current collected from a plasma can be described by the equation $I_e = J_0 A_s$, where I_e is the electron current, A_s is the effective surface area for electron collection (either the plasma sheath area or the area of a sphere with the limiting orbit radius), and J_0 is the electron thermal flux, given by

$$J_0 = (ne/4)(8kT_e/\pi m_e)^{1/2} = 2.68 \times 10^{-12}\, nT_e^{1/2} \text{ Amps/cm}^2, \qquad \text{(eqn. C.1.3.1.1)}$$

where n is the electron density per cm^3, and T_e is the electron temperature in eV. For example, in a "typical" LEO plasma of 10^6 electrons/cm^3 and a temperature of 0.1 eV, one could expect electron thermal fluxes of about 1.5 microamps/cm^2, or about 15 milliamps/m^2.

Electron current collection by wires is important in the case of electrodynamic tethers or when structures such as self-extending masts with wire braces are used. For instance, on ISS it was found that several square meters of electron-collecting wires on the array masts were connected to ISS ground. The array wing that was positive with respect to the plasma because of $\vec{v} \times \vec{B} \bullet \vec{l}$ effects (described below) acted as an electron collector, and became essentially grounded to the surrounding plasma. This complicated measurements of the vehicle charging due to solar cell electron collection.

An electrodynamic tether is a long wire orbiting in the Earth's magnetic field that uses the electric field generated by its motion, the so-called $\vec{v} \times \vec{B} \bullet \vec{l}$ field (where $\vec{v}$ is the velocity, $\vec{B}$ is the magnetic field, and $\vec{l}$ is the length of the tether or structure), to produce power or propulsion. This concept was proved on orbit by the Plasma Motor Generator (PMG) experiment, where both modes of operation were produced by emitting electrons (by means of plasma contactors) either at the top or bottom of a 500-meter tether to produce power (electron emission at the bottom) or propulsion (electron emission at the top). The maximum $\vec{v} \times \vec{B}$ on a structure in LEO is about 1/3 volt per meter.

In the case of the TSS-1R tether, its 20 km length produced a maximum of about 3500 V potential between its most positive and negative ends, since it was not oriented perfectly perpendicular to the velocity vector and the Earth's magnetic field. A satellite at its upper end collected electrons, and an electron gun at the lower end emitted electrons to complete the circuit. When the electron gun was not in operation, a large resistance prevented the Shuttle from being biased thousands of volts negative of its surrounding plasma. However, there remained a large voltage between the tether lower end and the Shuttle orbiter. This enormous bias eventually led to a continuous arc on the tether (see section C.1.2.3.1 below), which broke, freeing the satellite and ending the experiment. During the arc, the satellite collected over 1 amp of electron current to keep the arc going. Probe theory (Cohen et al., 1986) is usually used to calculate the total current collected by a wire with distributed potentials. However, before the break, TSS-1R demonstrated that a satellite at a high positive potential could collect an anomalously large electron current. See Zhang et al., 2000; Stone & Raitt, 1998; and Stone et al., 1998.

In the MSFC tether experiment, ProSEDS, the Propulsive Small Expendable Deployer System (Vaughn et al., (2004), the electrodynamic tether would be a bare wire, collecting current along its length, rather than just at its ends. In this case, arc mitigation requires, for example, graded insulation at the tether ends to eliminate the so-called triple-points where high electric fields can lead to arcing.

Electron collection in LEO is also affected by the vehicle plasma wake. Since orbiting LEO spacecraft are moving supersonically with respect to the ambient ions, there is a wake devoid of ions behind each spacecraft. The electrons that initially enter the wake build up a space charge that repels all other electrons, so the wake can be considered essentially devoid of electrons, compared to the ambient plasma. For most bodies, then, the only part that can collect ambient electrons is the ram-facing side. The Charging Hazards and Wake Studies (CHAWS) experiment (Cooke et al., 1994; Bonito et al., 1996) showed that a large body in LEO has a very deep wake, with a wake electron density of 10^{-4} of the ambient electron density or less, but with a temperature 10 times or so of the ambient, in agreement with earlier measurements by Raitt et al. (1984) and Murphy et al. (1986).

If a piece of conductive structure is surrounded by insulating material and is at a high positive potential relative to the ambient plasma, it could be subject to snapover (see section C.1.1.4.3 below), causing a greatly increased effective electron surface area, so the structure can collect an order of magnitude more current than one would naively suspect.

Insulating structure surfaces reach equilibrium potential with the LEO plasma of only a few volts negative, and do not thereafter collect current (Vaughn, 2003)

C.1.1.3.2 Ion Collection

While electrons are collected from all directions in LEO, spacecraft in LEO are moving supersonically with respect to the ions; therefore, ions are collected only by ram surfaces. In fact, since many conducting parts of a structure are far greater in dimension than the plasma sheath, the effective flux of ions to their surfaces is essentially equal to the ram flux of ions on their front-facing surfaces. That is, $F = n\ v$, where n is the electron (and ion) number density, and v is the spacecraft velocity. If we let A_{ram} be the ram-facing conductor projected area, and if we let I_i be the ion current and q the ion charge,

$$I_i = q\ n\ v\ A_{ram}, \qquad \text{(eqn. C.1.1.3.2)}$$

which for LEO circular orbit becomes $1.2 \times 10^{-15}\ n\ A_{ram}$ amps. For a density of about $10^{12}/m^{-3}$, this gives a current of about 1 mA/m^2. This, then, is a convenient rule of thumb for LEO ion current, about 1 mA per square meter.

Notice that for most purposes, the collected ion current depends only on the electron (and ion) density, whereas the electron current depends on the electron temperature, as well. To first order, then, when there is a current balance condition determining the floating potential, only changes in the electron temperature will cause changes in the floating potential.

Insulating ram surfaces will float at a potential such that the ram ion and thermal electron currents are equal, or only a few volts negative at the most.

C.1.1.4 Current Collection by Solar Arrays

C.1.1.4.1 Electron Collection

Electrons can be collected on positively charged cells of solar arrays by the cell interconnects, wiring traces, or cell edges. Solar array electron collection is intimately related to parasitic power drain, which is treated later in this document. However, here the discussion will be in more general terms.

For arrays that have fully exposed interconnects, cell edges, or power traces, electron collection is similar to that for wires or small spheres of the same total collecting area as the exposed conductors. One significant difference is that many solar cells have insulating coverslides. Since solar arrays by definition generate a voltage across each string, some of the solar cells, interconnects, or wiring will be at very different voltages than other parts. If a solar array string has 400 silicon solar cells in series, for instance, one end of the string will be about 200 V more positive than the other. The total electron current collected will be the integral of the collection of all the cells at their respective potentials away from the plasma potential. This depends, of course, on what the system ground is, and what the floating potential of the system is. Wherever the system floats with respect to the ambient plasma, only the cells and traces with positive potentials will collect many electrons.

If the array's exposed conductors are partially hidden from the ambient plasma (such as being underneath overhanging coverslides or between closely spaced solar cells), the coverslides can change the electron collection greatly. It has been shown that a coverslide with an overhang at least as big as the cell-plus-adhesive thickness will block electron collection at the cell edge very effectively, cutting it by a few orders of magnitude. Also, cell edges on cells that are separated by less than about 32 mils have greatly reduced electron collection (Chock, 1991b). One way of thinking about this reduced electron collection is that it becomes difficult or impossible for thermal electrons to "make the turn" to be collected at the cell edges. For such solar arrays, it is often the case that the lower the ambient electron temperature, the greater the electron collection, since more of the ambient electrons can "make the turn." This is the case for the ISS arrays, where the greatest amount of electron collection, and thus the worst system charging, occurs when the ambient electron temperature is the lowest.

It is possible for the solar arrays to undergo snapover if they are at high enough positive potentials. (See appendix C, section C.1.1.4.3 for details.) It is believed that snapover depends on the secondary electron emission characteristics of the solar array insulators. Contamination and/or texturing by atomic oxygen can decrease snapover. In ground tests, oil contamination was seen to prevent snapover completely on some samples. If snapover does occur, it is possible for the solar array to have an effective electron collection area as great as its entire geometrical area, rather than the tiny fraction of the array area that is normally occupied by interconnects or cell edges.

The solar array itself can provide a wake to block its own electron collection. For a sun-pointing array in equatorial LEO, the electron collection will be at a maximum near sunrise, and will shut off about noon when the array goes into its own wake. Of course, at night when the plasma is not dense and the array is not generating voltage, electron collection will be minimal. Thus, solar array electron collection in LEO is only important, and can only lead to a great deal of system charging, for about 1/3 of each orbit (the morning side).

C.1.1.4.2 Ion Collection

Snapover does not occur for ions, and the ion collection for solar arrays is almost always a linear function of negative voltage. Again, the total array collection is the integrated value of all negative cells at their respective potentials away from the ambient plasma, but for most solar arrays, this collection is small compared to ion collection from the structure. In the case of ISS, for example, Ferguson and Gardner (2002) could completely ignore solar array ion collection in modeling the ISS floating potential. When the array is in its wake, ion collection is further reduced.

C.1.1.4.3 Snapover

The phenomenon of snapover was observed in the early 1980s when power system designers first began experiments with high-voltage arrays. Although the process is broadly understood, many of the details are controversial and remain an active area of research.

Suppose a flat conducting plate is covered with an insulator and in this insulation there is a pinhole. If the plate is biased by a power supply and placed in plasma, it will collect current. For low voltages, current collection will be linear with bias voltage. Although the remaining surface cannot collect charge, it nevertheless is the source of an increasing electric field. This field results in ion bombardment of the insulator and secondary electron emission. The result is a rapidly growing sheath that collects charge and funnels it effectively to the pinhole. What is observed then is this: As voltage is increased from zero, current is collected linearly. At some point, current collection increases exponentially and finally saturates at a current level that is approximately the same as if the entire plate were conducting. On a solar array, the interconnects, wire traces, or cell edges act like pinholes; they are the conductors to which the current is funneled. The solar cell substrate and/or coverslides act like the insulator in the above example; they are the dielectric that furnishes the secondary electrons, and they act as a current-collecting plate.

The phenomenon is quite striking with conventional solar array designs and is easily observed in plasma test chambers. Here these are solar cells that are covered by insulating coverslides connected to each other by small, exposed metallic interconnects. At low voltages, the interconnects collect current roughly linearly with voltage. At around 150-200 V, the onset of snapover can be observed and by about 600 V the array is fully snapped over.

Avoiding snapover has become a major design issue. Strategies include insulating all surfaces, where practical, and choosing insulators with low secondary electron emission yields. While simply insulating all conducting surfaces provides initial protection, cracks or pinholes are difficult to avoid when materials must withstand years of exposure to harsh space conditions. It

should be noted that pinholes in high-voltage insulation usually expand as the large current density funneled through them destroys additional material. On the other hand, experience has shown that cracks or pinholes, if much smaller than the Debye length in the plasma, do not snap over. ($\lambda_D = 743(T_e/n)^{1/2}$, in cm, where T_e is the electron temperature in eV, and n is the electron density in cm^{-3}. (See eqn. D.2.3.1 in appendix D, section D.2.3.1. For LEO conditions, λ_D can be as small as 0.1 cm.)

As an example of a snapover-like effect on real solar arrays, consider the data in figure 1. The Advanced Photovoltaic Solar Array (APSA) was a very lightweight design proposed for widespread use in the early 1990s. Originally designed for deployment in GEO, the blanket material was carbon-loaded Kapton®, which had sufficient conductivity to avoid the differential charging that is a common problem in that environment. Proposals to adapt APSA technology to LEO recognized that atomic oxygen would destroy the blanket material within a matter of days. The LEO prototype was therefore designed with a blanket of Germanium-coated Kapton®, which would be resistant to atomic oxygen attack. This material is not as conducting as carbon but is still a weak conductor.

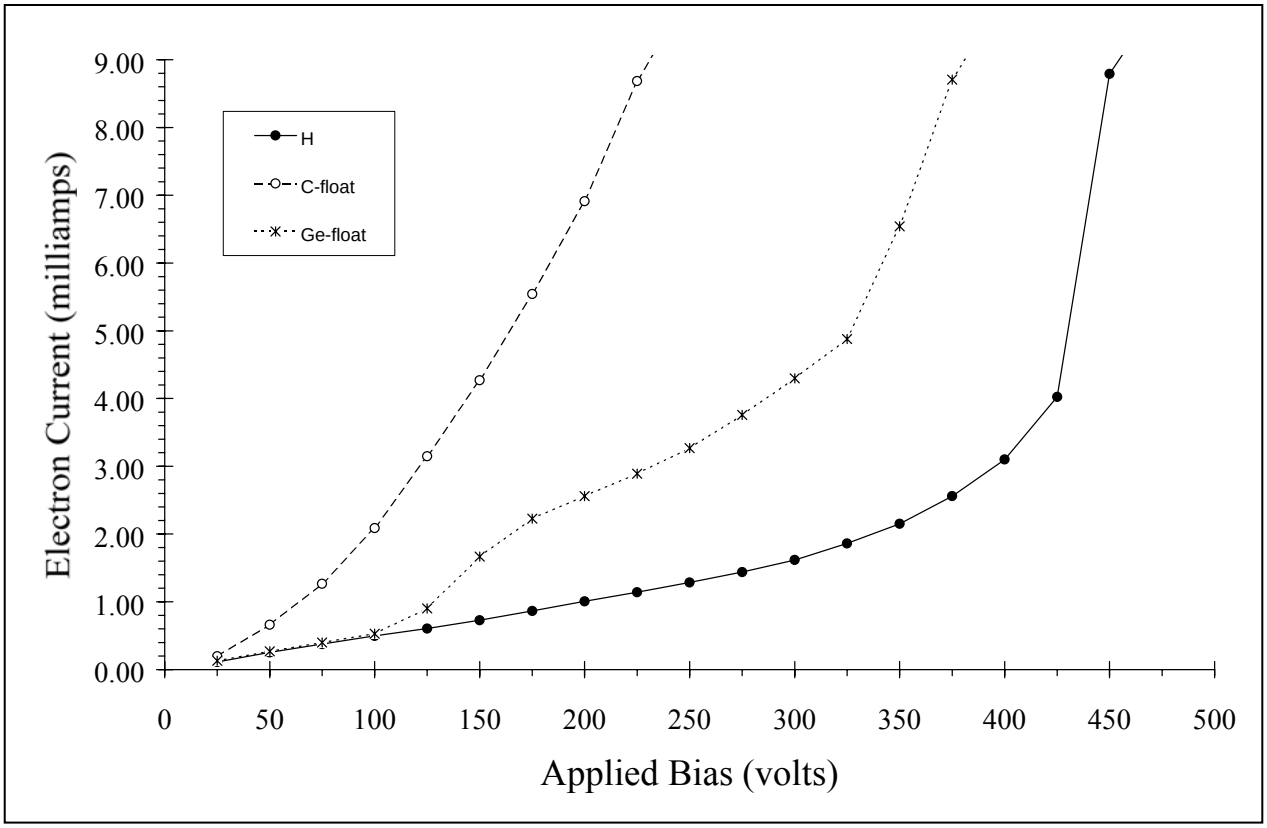

Figure 1—Electron Current vs. Bias for Three Solar Array Blanket Materials (Hillard, 1994)

Three sample coupons were constructed that were as close to identical as possible except for the blanket material. One was made from uncoated Kapton®, and the other two had blankets coated with Carbon and Germanium, respectively. They were tested in a space simulation chamber for current collection as a function of applied bias voltage. As the results show, the highly insulating Kapton®-H, shown in figure 1 by the curve designated "H," collected current linearly until around 300 volts. Current rose rapidly until about 400 volts when it became exponential, the signature of snapover. The weakly conducting Germanium-coated blanket collected linearly only until about 125 volts when it began its rapid rise, and the much more conducting Carbon blanket collected exponentially almost from the beginning. These experiments showed that the blanket itself could become involved in the snapover process and pointed to the critical need to test all proposed array coatings for plasma effects (Hillard, 1994). That is, with conductive blankets, the inherent conductivity can substitute for the secondary electron-induced conductivity to give snapover even at low voltages.

C.1.1.4.4 Parasitic Power Drain

Current collection from solar arrays or other conducting surfaces not only poses the threat of damage to the surfaces involved, but also can reach levels that result in a significant loss of power. Many efforts have taken place over the years to use the basic equations of plasma physics to estimate the magnitude of this loss, and one of them is presented here to illustrate the effect.

The high-voltage solar cell array for a high-power satellite looks more like a sheet electrode than like a spherical probe. K. L. Kennerud developed a method of analyzing the leakage current from such arrays based on fundamental equations developed by I. Langmuir (Kennerud, 1974). Kennerud's technique converts the linear array into a sphere having the same area, and then calculates the radius of the electron sheath surrounding the array. His experiments with small, positively charged solar-cell panels correlated well with his predictions.

Kennerud's results, shown in table 2, can be used to understand how the effect scales with altitude for the hypothetical solar array that he used.

Table 2—Leakage Current from Positively Charged Solar Arrays (Kennerud, 1974)

Array Altitude (km)	Electron Density, N_e (cm^{-3})	Electron Temperature (K)	Leakage Current		Power Loss, percent of Generated
			nA/cm^2	A per 1500V String*	
500	$6x10^5$	3,000	824.5	0.8494	7.72
700	$2x10^5$	3,000	274.8	0.2831	2.57
1,000	$7x10^4$	3,000	96.19	0.0990	0.90
2,000	$2x10^4$	3,200	28.38	0.0292	0.265
30,000	$1x10^2$	13,600	0.29	0.0003	0

* The string is 0.404 m by 255 m, with an area of 103.02 m^2.

Such rough calculations fail when the geometry becomes more complex. In particular, solar arrays with hidden interconnects such as the ISS arrays can collect current very differently from one with exposed interconnects. The ISS solar arrays, counter to intuition, collect more current at low electron temperatures than at high electron temperatures. Models have shown this phenomenon is caused by an electric field barrier to high-energy electrons. However, modeling electron collection by using spheres of equivalent "effective" area is very useful, and is incorporated in computer codes such as Environmental WorkBench (EWB), for instance. Modern computer codes, such as the NASA Charging Analyzer Program (NASCAP) series described below, will provide accurate estimates of parasitic power loss for any geometry. At high positive potential, snapover can make a solar array appear to be completely conductive. In addition, if a glow discharge caused by neutral gas ionization occurs on the array, the current collected can shoot up to tremendous levels (Ferguson et al., 1998; Vayner et al., 1999). Finally,

electric propulsion thrusters or plasma contactors, if placed in the vicinity of solar arrays, can short-circuit the plasma collection circuit and constitute a significant drain on the system power supply.

C.1.1.5 Current Collection at High Frequencies

In general, little work has been done on plasma effects involving high frequency power systems. While significant new effects are not expected, most parameters of interest such as corona inception and extinction voltages are expected to exhibit frequency dependence. One effect did emerge in the early 1990s concerning insulated conductors energized with 20 kHz AC that were exposed to LEO plasma conditions (Button et al., 1989). This work was underway because Space Station Freedom was originally designed to use such a power system. Research was suspended when the Space Station was reconfigured to use DC power.

If a conductor energized with low frequency AC is placed in LEO plasma, electrons are attracted to the insulating surface during the positive part of the cycle. These electrons "stick" to the material with a characteristic energy and are not repelled when the polarity changes to negative. Ions, however, are attracted during the negative part of the cycle and neutralize the electron charge for no net effect. At high frequencies. this neutralization process does not occur. Highly mobile electrons are still attracted during the positive part of the cycle but ions, because of the much larger mass, cannot respond to the rapidly changing field. The outer surface therefore charges to a negative potential close to the peak voltage on the power system waveform and remains charged.

Although ions cannot respond to the rapidly changing voltage waveform, they do respond to the buildup of negative charge on the surface. The resulting ion flux results in equilibrium where the surface is charged, as a rule of thumb, to about 90 percent of the peak voltage level used in the system. For a high-voltage system, ions will easily acquire sufficient energy to sputter material from the insulation. Such charging can have a number of other implications that could include an arcing hazard, depending on where such surfaces are located with respect to other conductors.

C.1.1.6 Wake Effects

Because a LEO spacecraft is supersonic with respect to the ions it flies through, a wake, essentially devoid of plasma particles of both signs, will form behind it. In LEO, the ambient ions are traveling at a thermal speed of about $9.79 \times 10^5 \, (Ti/m_i)^{1/2}$ cm/s, where Ti is the ion temperature in eV, and m_i is the ion mass in AMU (atomic mass unit). For a Ti of 0.2 eV (typical) and $m_i = 16$ (atomic oxygen), this gives an ion speed of about 1.1×10^5 cm/s, and a Mach ratio of about 5 for LEO orbit. Thus, the wake of a large body will extend as a cone about five times as long as it is wide. In this region (a sort of umbra), ion and electron densities will be severely depressed, and the remaining plasma will be at a high temperature (perhaps ten times that of the ambient plasma). In a surrounding region (a kind of penumbra), bounded by the shock wave, the plasma will be disturbed, but it is believed that the major effect will be hotter electrons than ambient. Beyond the penumbra, the plasma will be normal (Ferguson, 1985). Measured details of wake structure can be found in Raitt et al. (1984) and Murphy et al. (1986).

Instruments to measure plasma parameters in LEO should be placed beyond the plasma sheath surrounding the structure (normally a distance of 0.3 to 0.6 meters will suffice) and outside the wake of any structural element. In the case of the floating potential probe (FPP) on ISS, a compromise position was chosen that placed FPP outside the umbra of any structural element and on a pole to place it outside the plasma sheath, but it could not be placed out of the penumbra of some structural elements. Resulting plasma temperatures measured by FPP are considered to be higher than ambient temperatures, but the plasma densities seem reasonable. For instruments in such suboptimal placements, calibration must be done to convert measured parameters into ambient values, and such work is now proceeding with FPP. For a detailed discussion of wakes of large and small bodies orbiting in LEO, see Samir et al. (1986). For detailed scientific information about wake structure, see the works of N. H. Stone, who has devoted much of his life to researching this topic.

C.1.2 Arcing

C.1.2.1 Solar Array Arcing

C.1.2.1.1 Background

Until recently, the majority of spacecraft primary power systems used solar arrays and rechargeable batteries to supply 28 V. The choice of 28 V for the main bus voltage was made to take advantage of long-existing standards and practices within the aircraft industry. Plasma interactions at 28 V have not been generally considered a degradation factor of consequence. The only noted exceptions to their benign nature have occurred under extreme environmental conditions, especially during geomagnetic substorms for spacecraft operating at high inclinations. For low inclination spacecraft, i.e., those that completely avoid the auroral oval, 28-V systems have not been observed to arc.

As the power requirements for spacecraft increased, however, high-voltage solar arrays were baselined to minimize total mass and increase power production efficiency. With the advent of 100 V systems in the late 1980s, arcing began to be observed on a number of spacecraft.

Solar array arcs are generally characterized by the following parameters.

a. Breakdown voltage – The voltage required to initiate an arc depends on the plasma flux density, the system bias voltage, insulation, and construction and arrangement of the solar cells and solar cell strings. Breakdown voltage for a well-designed solar array can initiate as low as 75 V (negative biased) for spacecraft operating in a LEO plasma environment. Vayner et al. (2001) have shown that arc thresholds lower than about -300 V are invariably due to surface contamination with water and/or other contaminants.

b. Temporal profile – The time from initiation to maximum current can be from a fraction of a microsecond to seconds, depending on the power source and the circuit impedance. The total duration of an arc can be from microseconds to indefinitely sustained.

c. Current profile – The arc current can be as large as 100 to 1,000 amperes depending on the capacitance of the solar array. See figure 2, from Snyder (Purvis et al., 1984).

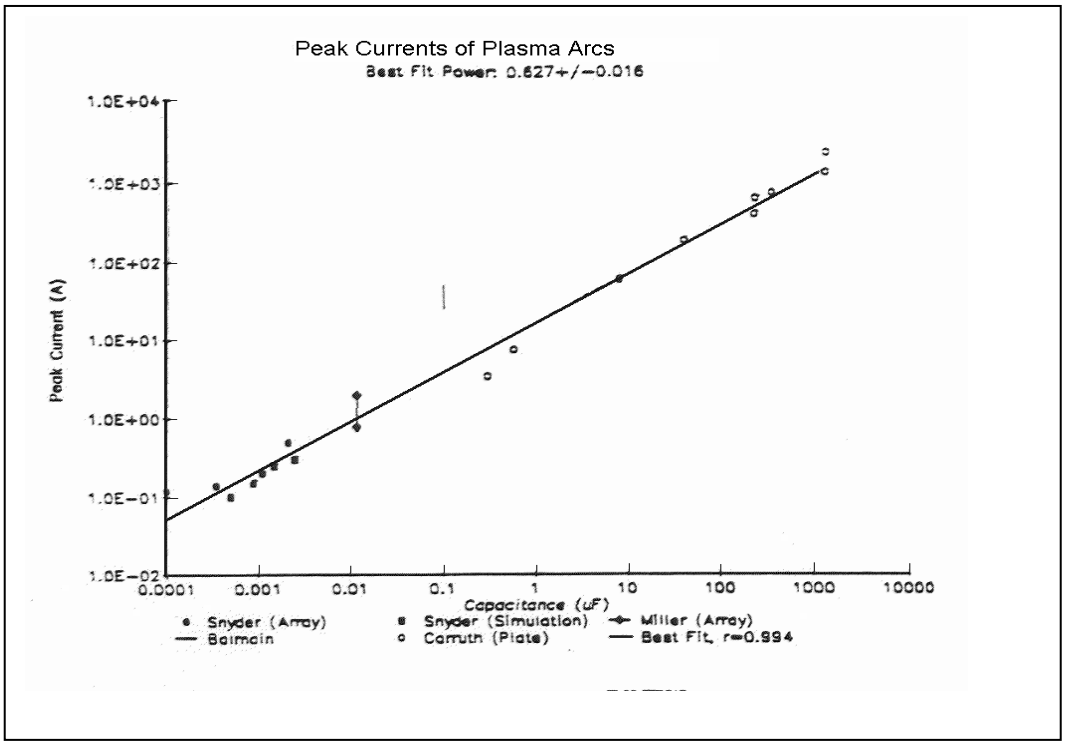

Figure 2—Peak Arc Current vs. Capacitance (Purvis et al., 1984)

Although many different taxonomies have been proposed for classifying arcs based on combinations of the above properties, these have generally been the work of physicists and have been designed to clarify issues for further research. For the design engineer concerned with risk mitigation, the following is a simpler scheme that assigns arcs to only two categories.

(1) Fast transients (primary or trigger arcs): The most common solar array arcs that are characterized by rapid rise time followed by extinction in a time that is several times the rise time. The critical parameter is that the energy involved is stored in whatever capacitance is available. The available capacitance can vary from a single array string to the entire spacecraft, depending on design. These arcs give rise to electromagnetic interference (EMI) but otherwise are not generally associated with significant permanent damage on small spacecraft. On ISS and other high-power systems, however, the energy stored in the capacitance electrically connected to the arc site could cause significant damage to a solar cell or power trace. Of course, repeated arcs at the same arc site can lead to degradation and failure even if the individual arcs are not very energetic.

(2) Sustained arcs (continuous arcs): Events that have been attributed with the destruction of on-orbit solar arrays. Generally, the process begins with a fast transient (a so-called “trigger arc”). Under some conditions, the transient develops

into a long-lived arc that is fed directly by the entire array, effectively becoming a short-circuit. Such events (called "sustained arcs") invariably involve large quantities of energy and can be severely damaging to cells, interconnects, or power traces.

Each of these will be discussed in more detail in sections to follow. Since all events begin as a fast transient, and most do not evolve beyond this phase, this type of arc has been the object of the most research in solar array arcing. The more destructive continuous arc has only been observed in the past few years as power levels have increased (causing higher and higher string voltages to be used). In addition, the drive to ever-more-compact string layouts has resulted in some unfortunate design choices. The sections that follow are therefore organized around the fast transient event. The continuous arc will be addressed in the final section with a summary of what is known at this time.

C.1.2.1.2 Initia tion Mechanism

The initiation of a solar array arc depends on the presence of a strong local electric field. Frequently, the source is an exposed interconnect which, depending on its location in the string, can be at high potential.

Most problematic are arcs that initiate at triple-points. A triple-point is a point in space where insulator, conductor, and plasma all meet. For a solar cell operating in LEO, this is usually the solar cell interconnect, but it can also be the edge of the solar cell (near the substrate or the coverslide). It has been shown that arcing on solar arrays at voltages less negative than about -1000 V is always mediated by the presence of a plasma. Identical samples to those that arced at -100 V in a plasma have been shown to withstand -1000 V bias in a pure vacuum. Arcs that occur in a pure (plasma-free) vacuum are called "vacuum arcs." Succeeding paragraphs discuss theories for the triple-point arcs that occur only in plasmas.

Arcs have been observed at relatively low potentials (as low negative as -75 V) when conductor surfaces are biased negative near insulator surfaces in the presence of a plasma. Arc rate is strongly dependent on plasma density and on coverslide temperature, which affects the surface conductivity. It can range from intermittent (on a scale of minutes and perhaps hours or longer) to several per second. Arc currents observed in ground tests are on the order of an ampere and can last several microseconds. These characteristics depend on the capacitance to space, increasing with increasing capacitance. These arcs are usually associated with solar cell array interconnects, but have also been observed on biased conductor surfaces covered with dielectric strips. They are likely to be of concern whenever conducting surfaces at negative potentials with respect to plasma abut insulating surfaces.

Several mechanisms are proposed for initiation of the arcs. Because much higher voltages are required to initiate arcs in a pure vacuum than in plasma, the plasma arc must not be a so-called vacuum arc, but is initiated at much lower electric field strengths. One favored mechanism proposes that a thin layer of relatively insulating film develops on the conductor. High electric fields develop across the film, caused by ion collection on the exposed face. The resulting electric field across the film causes electron emission from the conductor through the film into the plasma (Jongeward et al., 1985). A second, though perhaps related, mechanism assumes that the high electric fields at the edge of the dielectric cause propagation of secondary electrons to

the dielectric surface from near the conductor-dielectric-vacuum interface. Also, sufficiently intense electric fields can develop locally at the tips of structures built on the conductor surface because of the mobility of surface atoms driven by the electric field resulting from the presence of the nearby dielectric surface. However, this "structure related" arcing requires thin whiskers that have not been seen on realistic samples. Finally, gas desorbed from dielectric surfaces by electron impact can become ionized and serve as an ideal current path for the full-fledged arc.

At this time, no complete theories exist for the arc mechanism on solar cell arrays in a plasma. All require inclusion of an empirical factor to produce the observed low arcing voltage thresholds at triple-points. Experimental evidence indicates that an electron emission mechanism plays an important role in producing the arcs. A preliminary theory has been advanced that relates electron emission to the charging of a "dirty" layer on metal surfaces and the electric fields near an insulator-conductor-insulator surface configuration. This theory accounts for some of the experimental observations.

An electron emission mechanism for solar array arcing is consistent with several experimental observations. Kennerud (1974) observed that the apparent ion collection of a solar cell array was enhanced by an order of magnitude prior to arcing. This could be accounted for either by electron emission, or by an increase in ion density of the plasma. Snyder and Tyree (1984) observed this emission as an increase in electron current collected by sensors in the tank with the solar array. They also noticed that these currents did not cease when the plasma generator was turned off. Arcing could still occur with no plasma in the tank as long as these emission currents were detected. Snyder (1984) also noticed that arcs did not take place in a very low-density plasma (10^2 cm^{-3}).

The occurrence of arcs can be predicted from the potential of the solar array coverslides relative to the plasma. In a very low-density plasma, even at relatively high bias voltages, the coverslides remained near plasma ground and no arcs occurred. At higher plasma densities, the coverslide potentials became several tens of volts more negative than plasma ground. When this condition existed, arcs occurred. Electrons from the plasma do not have enough energy to pass through the energy barrier set up by the biased interconnects and reach the insulator surfaces (Parks et al., 1986). Electrons emitted from the interconnects of the array cause the coverslides to charge negatively relative to the plasma. These observations indicate that electron emission is necessary before the current pulse of the arcs can occur. Galofaro et al. (1999) have shown that an arc is always preceded by a nanosecond burst of electrons from the arc site. This burst can also ignite arcs on nearby surfaces.

Jongeward et al. (1985) proposed an arc mechanism model to account for this emission. The negatively biased interconnects tend to collect positive ions from the plasma. A layer of relatively high resistance material several angstroms thick can collect a sufficiently high surface density of positive ions to permit field emission of electrons from the region. This mechanism was first proposed to account for enhanced secondary electron yields from oxide films (Malter, 1936). Electrons emitted from this site are accelerated by the electric field between the cell or interconnect and the coverglass surface and strike the coverglass edge, which then emits secondary electrons in a cascade. Adsorbed gases are desorbed by electron impact. Ionization of these desorbed gases produces a dense plasma which is necessary for large currents to flow (Cho

& Hastings, 1991). Some inferences can be made that are consistent with the experimental observations. There must be enough ion flux to the interconnect to maintain a high surface charge on the high resistance layer. The metal-insulator geometry provides a focusing effect which increases the ion flux to the interconnect and maintains the surface charge density. Field emission accounts for the relatively steady emission, which probably represents a metastable situation. The solar array arcs arise when this stability breaks down, producing increased electron emission.

This model predicts the time duration and current of the arcs to almost a factor of two. Progress is also being made in predicting arc rates using this model. For instance, Perez de la Cruz et al. (1996) were successful in modeling the arc rates and thresholds seen in the SAMPIE experiment. The importance of adsorbed contaminants has been experimentally verified by Vayner et al. (2002).

Brandhorst and Best (2001) have shown that solar array arcs can be initiated in the laboratory by simulated micrometeoroid strikes.

C.1.2.1.3 Arcing Threshold

In an attempt to consolidate all known arcing information on solar arrays, Ferguson (1986) has analyzed the arcing data from the Plasma Interactions Experiment II (PIX II) array and compared it to other ground and flight data (see figure 3). Figure 3 is reproduced in Hastings (Hastings et al., 1992; Hastings, 1995) with theoretical predictions superimposed. The ground and flight data reported there is from Ferguson (1986). Ferguson's conclusions are listed in a-g below. Parenthetical material has been added to Ferguson's original conclusions.

a. A threshold for arcing of 2x2 cm solar cells into the plasma appears to exist near -230 V (with respect to the plasma). A threshold can exist for 5.9x5.9 cm cells at a lower voltage, but is not yet proved. (More modern studies have found thresholds as low as -75 V for specific array designs. The difference in threshold is more likely caused by coverslide thickness than by cell size.)

b. The arc rate at voltages above the threshold seems to be a power law of the voltage. This, combined with a nearly linear dependence of arc rate on plasma density, produces an apparent "threshold" which varies with plasma density. (Here, "above" means for voltages more negative than the threshold voltage. The apparent threshold is just because the "waiting time" for an arc to occur has exceeded the measurement interval.)

c. The arc rate decreases to a steady value on a timescale of a few hours. It is not yet clear whether this is caused by repeated arcing or by exposure to the plasma. (Further studies have shown (Vayner et al., 2002; Galofaro et al., 2002) that this is caused by both — outgassing into the vacuum removes contaminants over time, and arcs destroy contaminant islands in their burst of plasma.)

d. The arc rate can depend on the plasma density to the first power, on the square root of the ion temperature, and inversely on the square root of the ion mass. (That is, on the ion flux onto the sample.)

e. No significant dependence of the arc rate on the number of cells or interconnects could be found in the data. (This is still the case—the most likely arc site goes first, but there is no dearth of other arc sites when the charge builds back up. That this occurred in the data showed that each arc nearly completely discharged the available capacitance. Schemes can be proposed to prevent an arc from communicating with other cells or strings than the one on which it occurs, but in general all electrically connected cells or strings will contribute capacitance-stored energy to the discharge.)

f. The arc rate is greater in flight test conditions than in ground tests, possibly because of the atomic oxygen plasma in LEO. (It is unclear what other differences affect the arc rate, although cell temperature is clearly important in subsequent flight data such as Photovoltaic Array Space Power Plus Diagnostics (PASP-Plus.)

g. The arc rate in cells with exposed conductors on the backs, as in welded-through substrates, is higher at all likely arcing voltages than the rate for cells exposed to the plasma only on the fronts. (This effect could be caused by copper being exposed on the backs, as contrasted with silver on the fronts.)

Studies by Upschulte et al. (1994) and Hastings et al. (1992) confirm that a voltage threshold exists for solar array arcing, and for certain values of a parameter called the field enhancement factor (FEF) (Cho et al., 1990), reasonable values of the threshold are predicted. Vayner et al. (2001) have shown that arcing is enhanced primarily by the presence of desorbing contaminant layers, although thin coverslides and other geometrical factors can also enhance the electric field and lower the arc threshold. Snyder et al. (1998) have shown that hot arrays (100^{o} C) have a higher arc threshold than cool arrays (room temperature) in ground tests, presumably because the coverslides become more conductive at high temperatures. These results were confirmed on orbit in the PASP Plus experiment for the APSA-type solar arrays (Soldi & Hastings, 1995).

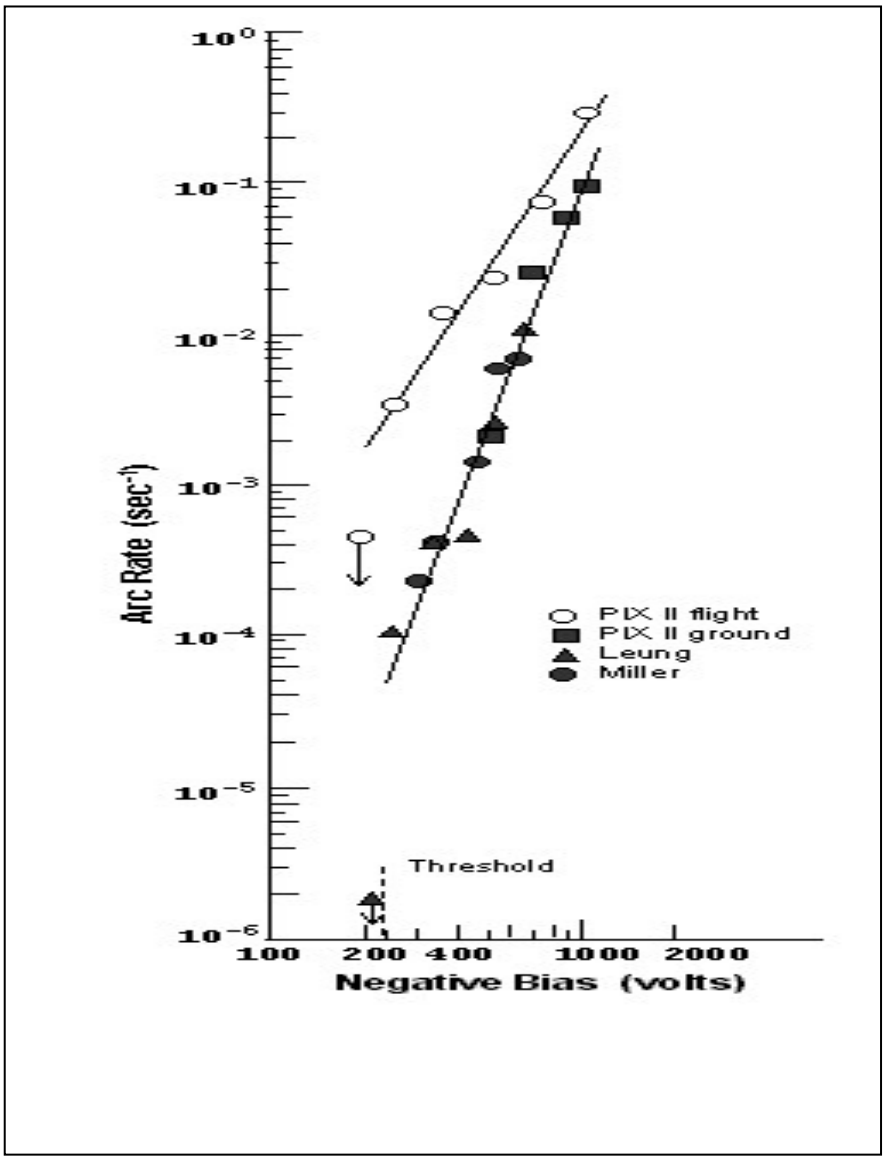

Figure 3—Arc Rate vs. Voltage for Standard Interconnect Cells
(Threshold is inferred from the plasma arcing measurements. Ferguson, 1986)

C.1.2.1.4 Typical Waveform

Figure 4 shows the time dependence of the current from an array segment during an arc (Snyder & Tyree, 1984). A typical arcing sequence has the following four regions:

I. The arc is initiated and the current increases to a peak value. The rise time varies from less than 0.1 μs to about 1 μs. The peak amplitude and rise time depend primarily on the capacitance electrically connected to the arc site.

II. The current then remains near the peak value for some time.

III. The current decreases with a roughly exponential decay. The decay time associated with the termination of the arc should not be confused with the total duration of the arc. During this decay, the current is space-charge limited.

IV. The arc terminates suddenly and the array begins to recharge to the bias voltage. At this point the coverslides of the array are substantially positive relative to both space and the arc point. The coverslides collect a substantial electron current from the plasma, resulting in the observation of a slight negative pulse.

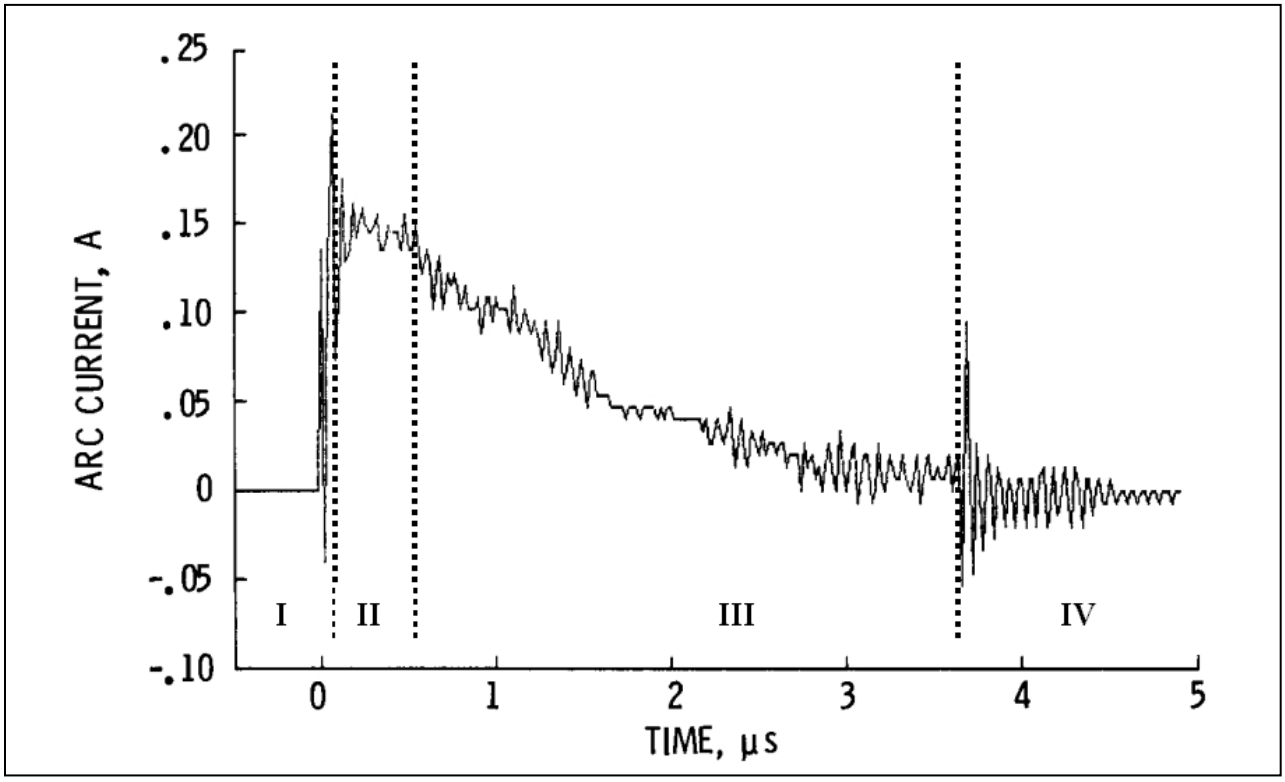

Figure 4—Typical Waveform for an Arc (Snyder & Tyree, 1984)

C.1.2.1.5 System Response

Arc currents can flow out into the surrounding plasma, with the return currents distributed over wide areas of other spacecraft surfaces.

During an arc two things will happen. As charge leaves during an arc, the potential of the arc site changes and the potential of the system, electrically connected to the arc site, will change. As a result of the potential change, return currents will flow to restore equilibrium. The return currents will come both from the surrounding plasma and from the arc-generated plasma. There are two impacts on other systems. The structure currents will look like noise to instrumentation. And the change in spacecraft ground will affect plasma currents to surfaces. In principle, these responses are the same for transients of any cause: docking, thruster firings, waste dumps, and beam experiments. Only the magnitudes will be different.

The response of a system to an arc can be estimated from a circuit analysis including terms to approximate the capacitances of the surfaces to space. An arc can be simulated in such a model by injecting an appropriate current pulse and computing the circuit transients (Metz, 1986).

C.1.2.1.6 Damage Potential

Initial indications that sustained arcs could cause substantial damage to solar arrays were obtained in testing where the bias power supply, intended to impress a potential difference between an array and its coverslides, was not sufficiently isolated from the sample when arcs occurred (see section C.1.2.3.1). Tests at Lewis Research Center (LeRC), now Glenn Research Center (GRC), in the 1980s showed that solar array interconnects could be melted by arc currents as large as 40 A (Miller, 1985).

Although pictures of damage produced by on-orbit sustained arcs are rare because most arrays that have arced are not recovered, we do have photos of damage suffered by the European Space Agency (ESA) European Retrievable Carrier (EURECA) spacecraft that was recovered by the Space Shuttle. Figure 5 shows a sustained arc site on its solar arrays. In this case, the sustained arc eventually burned through the array substrate to the grounded backing, completely shorting the array string to ground.

The Space Systems Loral satellites PAS-6 and Tempo-2 underwent sustained arcing in GEO that led to several shorted solar array strings and a severe loss of power. Although these were GEO failures, it is believed that after the initial arc occurs, the mechanism for sustained arcing is the same for LEO. Subsequent SS/Loral satellites underwent extensive modification to prevent sustained arcing, and have had no similar string failures since that time. These modifications were the following:

a. Changing the array layouts so that strings with high-voltage differences were not adjacent to each other.

b. Including blocking diodes to prevent high currents from flowing during an arc.

c. Grouting the cell edges on the strings with the highest voltage differences to prevent arcs from being sustained between strings.

A sustained arc on a test sample of arrays for the Earth Observing System – Morningside 1 (now Terra) (EOS-AM1) satellite, was seen in laboratory testing. Figure 6 is a frame from the videotape taken during the test, and figure 7 shows the vicinity of the site where the arc occurred. The capacitor used in this test to start the initial arc was 5 microfarads, and the arc started and continued until the power supply was manually shut off seconds later. The solar array string was completely shorted out. This test led to rework of the entire array strings on the Terra satellite to prevent arcing on orbit. Flat-pack blocking diodes were incorporated into each string to prevent high currents from flowing during an arc, and Kapton® tape was used to cover exposed power bus conductors. The modifications made to the EOS-AM1 and SS/Loral arrays are incorporated in NASA-STD-4005 section 4.1.5b.

Figure 5—Sample of Flight Array from ESA EURECA Mission after Sustained Arcing (Ferguson and Hillard, 2003)

Figure 6—Video Frame from EOS-AM1 Sustained Arc Test (Ferguson and Hillard, 2003)

Figure 7—Arc Site of Sustained Arc on EOS-AM1 Sample Array. Cells are 2x4 cm. (Ferguson and Hillard, 2003)

The most famous sustained arc event of all led to the breakage of the TSS-1R electrodynamic tether, and the loss of the attached satellite. Figure 8 shows the burned, frayed, and broken tether end still attached to the Shuttle after the break. Incidentally, the tether continued arcing long after it and its satellite were drifting free, until finally it went into night conditions where the electron density was insufficient to sustain the arc. Noel Sargent (2002) has investigated whether the high current and long duration TSS-1R arc was seen to disrupt Shuttle communications. Although he has found no record of disturbed communications during the event, for most of the time, the arc was shielded by metallic structures from the communications antennas, and when the tether broke, the arc was many meters from the receiving antennas. We do not know whether sustained arcs produce radio noise severe enough to be a communications problem.

Figure 8—The End of the Remaining TSS-1R Tether (Ferguson and Hillard, 2003)

When the structure or array capacitance electrically connected to the arc site is sufficiently large, the initial transient arcs themselves can be large enough to produce significant damage. Figure 9 shows an anodized aluminum plate that has undergone repeated arcing in the laboratory with the ISS structure capacitance attached. Its thermal properties have been completely destroyed, along with most of the insulating surface layer of aluminum oxide. Because it was not feasible to redesign all of the surfaces on ISS or all of the connections between surfaces to eliminate the enormous connected capacitance, a plasma contactor was baselined for ISS to prevent charging to arcing voltage levels.

Figure 9—Anodized Aluminum Plate after Repeated Arcing (Schneider et al., 2002)

C.1.2.2 Electromagnetic Interference (EMI)

Solar array arcs typically involve the violent discharge of very large currents for very short times. Not surprisingly, the electromagnetic spectrum associated with such discharges obeys the typical power law that has long been observed with arc discharges. An example of such a spectrum is shown in figure 10 (Leung, 1985). The test article was a small solar array sample that was proposed for a plasma interactions experiment in the Space Shuttle cargo bay. The test was designed to learn whether the radiated EMI from the sample would exceed orbiter specifications. The test was done with the bare array alone and with an added capacitance that simulated the energy storage associated with a full-size array. The biasing power supplies were electrically isolated from the arcs by a large resistor. As the curves show, even arcs from a small test array exceed allowed EMI specifications over most of the frequency range. It should be expected that arcing will always produce detectable EMI and that laboratory testing will be needed to quantify the level of interference. The magnitude of radiated EMI is a strong function of the "antenna gain" composed of those conductive (radiating) elements connected to the arc site. This effect heavily influences the shape of the radiated EMI spectrum (Sargent, 2002). Since antenna gain is extremely difficult to estimate, testing is essential.

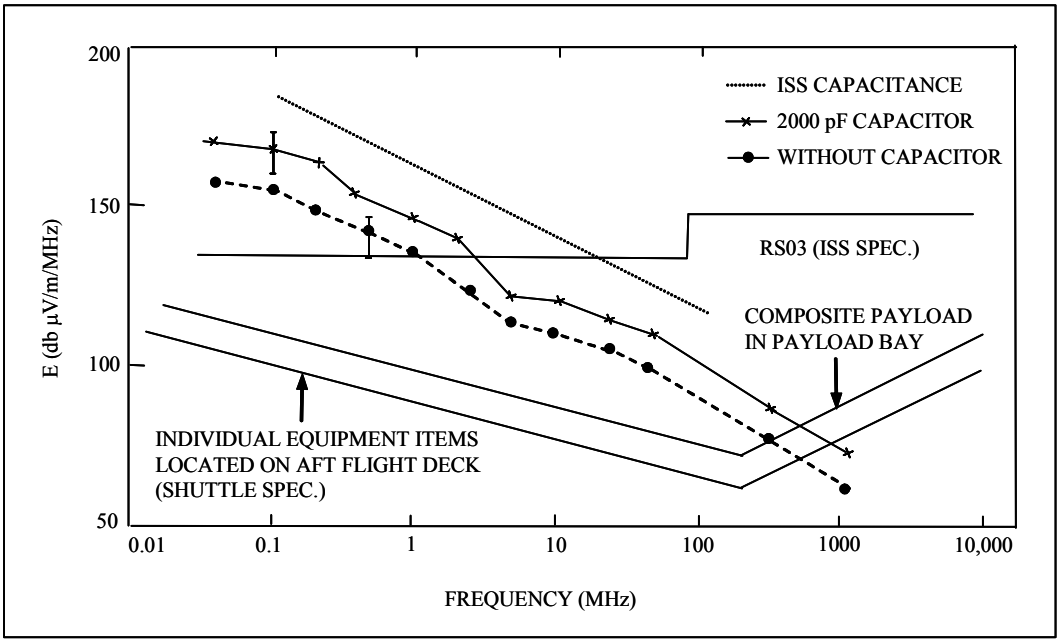

Figure 10—EMI from a Small Solar Array Arc and a Hypothetical ISS Anodized Aluminum Arc Compared to Orbiter's Specs (after Leung, 1985)

C.1.2.3 Structure Arcing

Generally speaking, there are two forms of structure arcing. The first is triple-point arcing, as has been discussed for solar arrays; and the second is dielectric breakdown. For triple-point arcing, an insulator must surround a highly negative conductor, and an arc can occur at the conductor-insulator-plasma conjunction, where the electric field is highest. Dielectric breakdown is completely different, and will be discussed below.

An insulator not in the wake in LEO will come through current balance to a potential within a few volts of the plasma potential. If that insulator covers a conductor, the conductor can be at a very different potential (such as the negative floating potential of the spacecraft, for instance). In this case, a thin insulator can undergo dielectric breakdown under the high electric field developed across it. While this can occur for any type of insulator, it is of perhaps greatest interest in the case of anodized aluminum, the main ISS structural element, and a material used in astronaut Extra-Vehicular Maneuvering Unit (spacesuit) (EMUs). Because the dielectric layer in anodized aluminum is typically very thin (0.1-1 mil), it can break down at potentials as small as -100 V or less—less than the negative floating potential that is possible for a 160 V array. It was the arcing threat from the ISS anodized aluminum that forced ISS to incorporate the PCUs to control ISS floating potentials. The PCUs act by creating a large localized plasma cloud that makes good electrical contact with the surrounding plasma, and essentially by brute force, grounds the ISS structure to the ambient plasma. A generic plasma-contacting device is called a "plasma contactor."

Different samples of anodized material break down at different potentials in a plasma (Hillard et al., 2000). Although ISS sulfuric acid anodize withstands about -200 V before breaking down, the chromic acid anodize was found in ground tests to break down at about -72 V. Most disturbing of all, chromic acid anodized samples for astronaut EMUs were found to break down at potentials of only -60 , relative to the plasma, with a two-sigma error bar of 10 V. It is thus possible that an astronaut, grounded to ISS by his tether or conductive tools, could undergo an arc at only -50 V. A sneak circuit analysis showed that such arcs could put > 40 milliamps of current through an astronaut's heart (Koontz, 2005). Since this amount is enough to cause heart stoppage, it is imperative that, if the ISS plasma contactors are inoperable during astronaut Extra-Vehicular Activities (EVAs) (spacewalks), a method be used to prevent ISS astronaut workplaces from floating more than 50 V negative.

Dielectric breakdown currents will essentially discharge all surfaces close enough (about 2 meters or so) for the induced plasma cloud to reach. For thin dielectric layers, a few square meters of surface are effectively a capacitor of many microfarads, and can hold several joules of energy, all of which can be discharged in the arc. For many ISS surfaces, peak arc strengths of hundreds of amps have been calculated. Arcs this strong will melt the arc site and spew molten metal through space. Plasma chamber tests of this kind of arcing are spectacular indeed! Arcs on one anodized surface have been seen to trigger arcs on nearby line-of-sight surfaces (sympathetic arcs; see Vayner et al., 1998).

Very thin dielectric layers will have a low enough resistance that for the purposes of the plasma, they would collect current rather than building it up on their surfaces. Thus, while mitigating dielectric breakdown, they must be considered as conductors rather than insulators.

Predicting arc thresholds for thin insulating layers is not as simple as using the published dielectric strengths for insulating materials. It has been found that identical thicknesses of the same anodization can differ by a factor of three or more in arc threshold voltage in a plasma. This can be caused by differences in sealing the anodized surfaces, which could affect their resistance to plasma currents. Until the theoretical situation is better understood, plasma testing must be used to determine the dielectric strength of insulators in applications, which could lead to charging in LEO (Hillard et al., 2000).

Carruth et al. (2001) have found that dielectric breakdown can also be initiated by simulated micrometeoroid strikes at voltages as low as -75 V. In tests at the Glenn Research Center, anodized aluminum plates were seen to breakdown in a simulated space plasma at voltages as low as -55 V (Galofaro et al., 1999).

C.1.2.3.1 The Continuous Arc (Sustained Arc)

Arcs that occur in air when electrical contacts are made or broken are caused by breakdown of the neutral gas (Paschen discharge). Although these can become continuous ("showering arcs"), they are not the same phenomenon as the continuous arcs in a LEO environment, which involve breakdown of the gas liberated by the arc itself. [See Holm (1999) for a discussion of continuous arcs in air.]

When the LEO arc circuit includes the solar arrays, distribution cabling, or other source of power, it can be possible for structure or solar array arcs to become continuous (or sustained). Such continuous arcs, fed by the power supply, have an essentially inexhaustible source of energy and can lead to catastrophic damage. This hypothesis for the loss of solar array strings on the SS/Loral satellites PAS-6 and Tempo II was confirmed by ground tests done by Snyder et al. (2000). Later testing on the EOS-AM1 arrays showed that continuous solar array arcs could occur in a LEO environment at a string voltage as low as 100-120 V. (In those tests, the sustained arc occurred at a voltage relative to the surrounding plasma of -250 V.) The most recent data (Vayner et al., 2003) has shown that strings with potentials as low as 40 V with respect to each other can lead to sustained arcing. The scenario for the catastrophic loss is given in Ferguson et al. (1999), and is summarized here as follows:

First, an ordinary solar array arc must get started, usually at a triple-point as described above. In the case of the SS/Loral arrays, the differential voltage between solar array and plasma could have been as low as 100 V, since the SS/Loral arrays were using thin coverslides similar to the APSA cells, which arced at voltages as low as -75 V on orbit. See the PASP Plus results in Soldi and Hastings (1995).

When the initial arc (sometimes called the primary or trigger arc) is generated, it discharges only the local capacitance, but the arc plasma expands out from the arc site and comes in contact with an exposed conductor at a very different voltage. In the case of the SS/Loral arrays, the most positive end of the array strings was less than a millimeter away from the negative end. Now the

arc plasma makes direct contact with the other conductor and makes for an almost dead short to that spot. The arc current has changed from one that is discharging capacitance to a current between two ends of the solar array string.

If the current available to the arc site from the functioning array is greater than a certain threshold value (believed to be about ½ amp for some array designs) and the voltage between strings is above a certain value (believed to be about 40 V for some array designs), the arc can become continuous. In ground tests, these arcs continued until the source of power was artificially turned off. In space, the arc would presumably continue until the exposed conductors were melted through and the circuit was thereby interrupted. This process could take seconds or minutes. Ground tests have shown that an arc that persists for more than a few hundred microseconds will not shut off by itself.

An arc that lasts long enough will locally heat the substrate and release gases. In the case of a Kapton® substrate, the Kapton® chars, but the char is also a good conductor, providing a path for the arc to continue. Snyder et al. (2000) have shown that the heat generated in continuous arcs on Kapton® is sufficient to produce the Kapton® charring measured after the event.

In any event, a continuous arc can destroy a whole string (if the arc is between traces on the same string) or adjacent strings (if the arc is between strings) or the entire array power (if the arc is between combined power traces). The possibility of losing the entire array power on the Deep Space 1 mission caused the builders to remove a solar panel that had already been installed to modify it and its sister array to prevent continuous arcing. Its power traces were only a few millimeters apart, and were exposed both to the plasma and to each other before the modifications were made. Afterwards, insulating material was used to prevent arc plasma from shorting out between the power traces.

Anodized aluminum structure elements can be subject to continuous arcing if the arc plasma generated can contact the solar array or other power source or if the potential at the arc site can be maintained at a high enough negative level by a high-voltage electron-collecting power source. Such continuous anodized breakdowns were called “sizzle arcs” by the team that discovered them (Murphy et al., 1992).

Finally, an arc on an electrodynamic tether can become continuous. The infamous arc on the TSS-1R tether that led to its break and the loss of the satellite was a continuous (sustained) arc with its power supplied by the tether. The arc site was a flaw in the tether insulation that spewed out gas, which became ionized and completed the arc circuit path (Szalai et al., 1996; Vaughn et al., 1997). Since in this case the power source was more one of constant voltage rather than constant current, the 3500-volt potential difference between the tether top and bottom caused the arc site to float at just the negative potential (about -600 V) necessary to keep the arc going and still collect the ~1 ampere arc current of electrons on the satellite. Had TSS-1R used a tether of greater resistance, the threshold arc current could not have been maintained. For example, a total tether resistance of 10,000 ohms would have limited the arc current to less than 0.4 amps, less than the sustained arc threshold. As an alternative, if the satellite electron collection capability had been limited to less than about ½ amp, the arc could not have been sustained. Of course, these measures would have severely restricted the power or propulsion that could be obtained by

tether operation and could not be tolerated on an experiment that was not just a proof-of-concept. An arc detection circuit could have also been used to shut the tether down at the satellite end when very large currents were first detected. One should never assume that a high-voltage power system will not arc.

APPENDIX D
MITIGATION TECHNIQUES

D.1 Current Collection

If a spacecraft has no exposed high-voltage conductors, it will not collect much current. That is, insulation or encapsulation is a valid technique for preventing current collection in LEO. The GEO Spacecraft Charging Guidelines (Purvis et al., 1984) recommend coating spacecraft surfaces with conducting materials to keep all surface potentials the same and reduce differential charging. In LEO, however, the space plasma will act to keep insulating surfaces at the same potential (discounting wake effects), so conductive coatings are not needed. If encapsulation or insulation is not possible, hiding conductive surfaces (like the edges of solar cells) from the ambient plasma by use of narrow spacing of overlying insulators (like coverslides) can choke off most current collection. It has often been remarked that if the ISS solar arrays had just a little more coverslide overhang and/or a little tighter cell spacing, the issue with ISS charging would not have occurred. Of course, if all high-voltage components are inside a sealed pressure vessel, they cannot collect current from the ambient plasma.

Encapsulation, or grouting with Room Temperature Vulcanized (RTV) rubber, of solar arrays has been shown to be an effective method to prevent electron collection and charging (Reed et al., 2001). Of course, the grout must be UV and AO resistant. Care must be taken in the use of encapsulants, however, when the possibility exists of outgassing in the presence of high-voltage components. For instance, on SAMPIE, one of the high-voltage power supplies was destroyed by a Paschen discharge that occurred on a high-voltage component where the encapsulant had delaminated and a neutral pressure was enclosed with the high-voltage component (Ferguson & Hillard,1997). (See figure 11 for Paschen curves.) On TSS-1R, the “trigger arc” was a Paschen discharge due to entrained gas inside the tether pulley casings (Szalai et al., 1996; Vaughn et al., 1997). In this case, a flaw in its insulation exposed the tether conductor.

Placing plasma-current-collecting conductors into the wake of a large spacecraft is an effective technique for preventing current collection. On ISS, for instance, FPP data showed that when the arrays were turned into their own wakes, they collected such a small amount of electron current that the ISS structure would not charge. On ISS, this technique of wake-pointing the arrays is now used as a backup for the Plasma Contacting Units during astronaut EVAs. Of course, very high potentials on wake-pointing conductors can collapse the wake, but this will require thousands of volts potential for large structures.

For a spacecraft that will often undergo auroral passage, one must be careful with the use of insulators. Like in GEO, spacecraft in the aurorae can undergo rapid differential charging on insulators, leading to buildup of potentials that might lead to arcing. It is hoped that a subsequent document will cover polar-orbiting spacecraft in the detail this document covers equatorial LEO orbits.

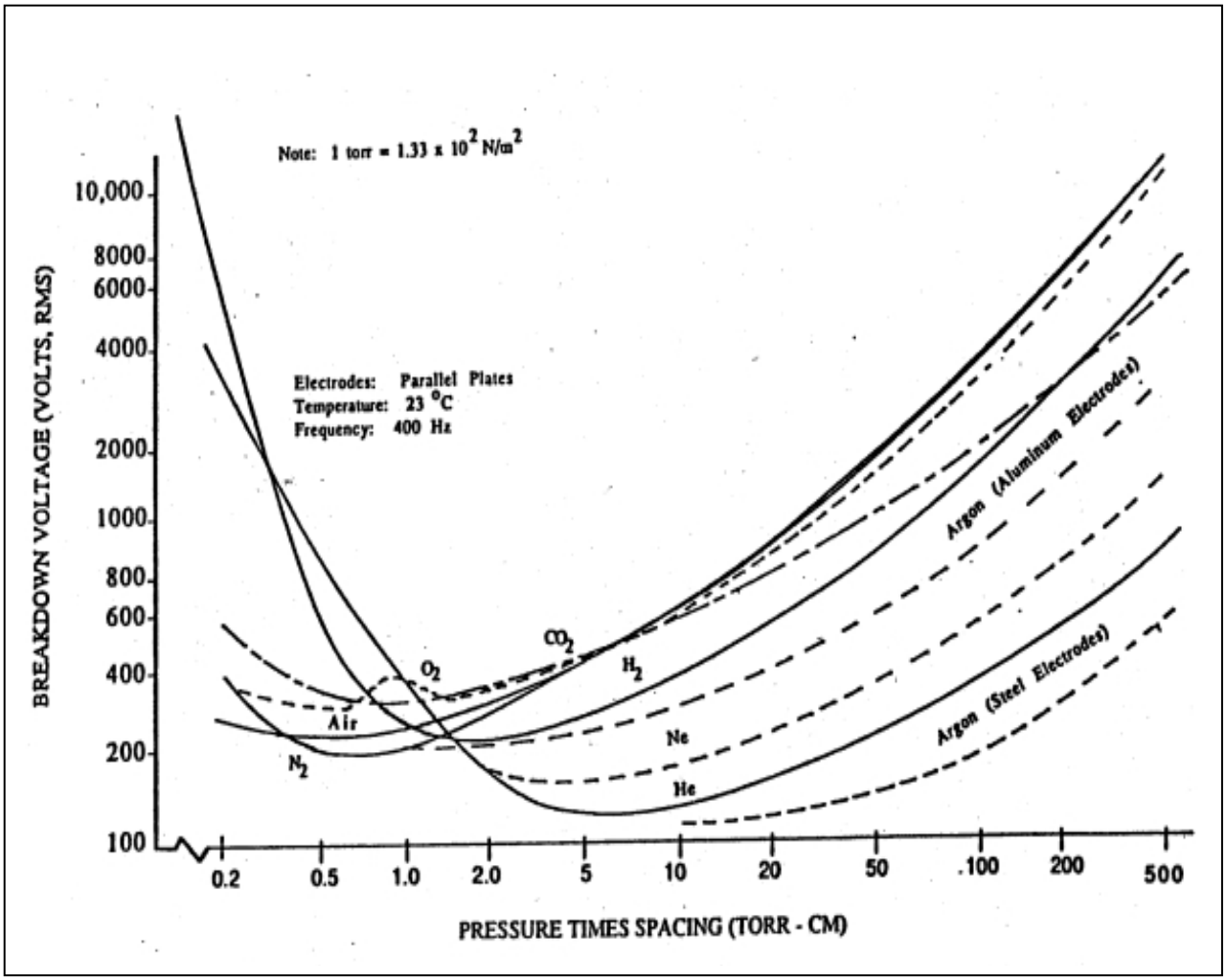

Figure 11—Voltage Breakdown of Pure Gases as a Function of Pressure Times Spacing (Paschen curves for different gases, from Dunbar, 1988)

D.2 Controlling Spacecraft Potential

There are three basic techniques to control spacecraft potential. One is to place the structure at the most positive potential generated by the LEO spacecraft power system (the positive ground option). The second is to ground the structure by brute force to the ambient plasma (the plasma contactor solution). The third is to prevent any plasma exposure of high-voltage conducting surfaces (the encapsulation solution). These mitigation strategies are discussed in order below. For ideas about other ways to prevent spacecraft charging, see Ferguson (2002).

D.2.1 Positive Ground

Since charging in LEO is dominated by current collection on the most positive end of the solar arrays, and the negative end floats at about 90 percent (typically) of the string voltage, the positive end of the array will be about 10 percent of the array string voltage away from the plasma potential. For a 160 V array, this means a positively grounded structure will float at 16 V or less away from the plasma potential. Most deleterious plasma effects are minimal at such a potential. In fact, the structure in this case contributes to electron collection, and actually floats closer to plasma potential than the positive end of the array does, taken alone, because of exposed grounded conductors on the structure.

However, most spacecraft power systems are negatively grounded because of a dearth of space-qualified electronics with the positive ground polarity. Although very efficient power management and distribution (PMAD) systems now exist that use buck-boost converters to change the ground polarity and voltage (Button et al., 2002), most spacecraft busses do not incorporate this technology yet.

For instance, when ISS charging possibilities were first being considered, it was estimated that to change the power system ground from negative to positive would cost at least $100 M. It was decided instead to use the plasma contactor mitigation strategy detailed below, which ended up costing less than $35 M.

A variant of this technique uses a center-tapped array, but will only cut the maximum structure potential to about half the solar array string voltage. Grounding the power system at about 90 percent of its maximum positive voltage would be nearly ideal, since it should place the spacecraft ground at near the plasma potential.

D.2.2 Plasma Contactors

A device that makes good contact with the surrounding plasma can effectively ground its point of contact. If the device is a large sheet of metal, it will dominate current collection and stay near plasma potential. However, the sheet of conductor must be much larger than the solar array effective electron-collecting area for this solution to work. In the case of ISS for instance, the metal sheet would need hundreds or thousands of square meters of ram ion collecting area to be effective. In LEO, the drag produced by such a large area would be prohibitive.

Electron guns were used on PIX-II and PASP Plus (Guidice et al., 1997) to emit the electrons being collected by high-voltage solar arrays and thus prevent charging, but such devices are limited by space charge considerations to low emitted electron currents. A better solution is a device that is not limited by space charge considerations, i.e., a plasma contactor.

A plasma contactor generates a high-density plasma cloud, which expands and makes good electrical contact with the ambient plasma. Usually, a hollow cathode device is used to emit a xenon plasma (Davis et al., 1986) whose space charge is nullified by nearly equal densities of electrons and ions in the emitted cloud. The very mobile electrons carry current into the surrounding ambient plasma. This current can be very large. For instance, the ISS PCU device

has a hollow cathode element smaller than a little finger, but can emit up to 10 amps of continuous electron current. In the case of ISS, the PCU acts like a ground rod at its location to effectively ground (to within about 20 V) the structure to the ambient plasma. Of course, at other points, the structure will still have the $\vec{v} \times \vec{B} \bullet \vec{l}$ potential away from the ambient plasma. In LEO, $\vec{v} \times \vec{B} \bullet \vec{l}$ amounts to a maximum of only about 1/3 V per meter, which is only about 40 V from end to end on the largest structure ever orbited (ISS), so at all points the potential is outside the arcing range (-50 V or less).

While a hollow cathode plasma contactor requires xenon gas vessels, refurbishment, etc., other devices with little or no expellant are being explored for use as plasma contactors. As an example, a plasma contactor made of microtips and microscopic holes, with an imposed bias, could theoretically emit electrons over a wide area and thus defeat the space charge limitation with no working gas. A patent has been awarded for using such a device to control spacecraft potentials in GEO (Katz, 2001), but making such a device work reliably in the high density plasma of LEO is no small feat and has not yet been done.

D.2.3 Encapsulation

Encapsulating the high-voltage conductors on solar arrays, etc., can have a two-fold beneficial effect. First, it can prevent arcing at triple-points by keeping the plasma away from the conductor-insulator junctions. Second, it can prevent electron collection by the arrays, and thus prevent spacecraft charging at its root cause. As of the year 2002, the only arrays ground tested in a simulated LEO plasma to withstand bias voltages greater than -300 V were those with the arrays or cells encapsulated (Reed et al., 2001; Brandhorst & Best, 2001; Ferguson et al., 2002). Since that time, other mitigation techniques have extended the arcing threshold to at least -500 V, but no arrays with unmitigated arcing have withstood more than -300 V to date.

When encapsulating arrays or cells, one must not ignore several caveats. First, no air must be entrained anywhere. While this seems obvious, at least one set of encapsulated test arrays sent to NASA's Glenn Research Center had sufficient air entrained that the coating delaminated and swelled under vacuum. In fact, so much air was entrained that the test articles under vacuum appeared to swell up like plastic balloons. In cases where only a very small amount of air is trapped, visible effects may not occur, yet the trapped air will present the danger of Paschen breakdown under high voltage (see figure 11).

Second, the encapsulant thickness must be sufficient to withstand dielectric breakdown at the highest array voltage. For thin-film arrays, this consideration can contribute significantly to the array mass. In keeping with the discussion on structure arcing, it is important that thin-film encapsulants be tested under voltage in a plasma environment, rather than relying solely on published dielectric strengths.

Third, the encapsulant must not be able to peel away from high-voltage components, or Paschen breakdown can occur because of entrained outgassing products that can reach sufficiently high neutral pressures. Figure 11 shows the Paschen breakdown curve for a number of gases for DC to low frequency AC (~ 400 Hz) for parallel plates (Dunbar, 1988). Here it can be seen that for a wide range of pressure distance combinations, the Paschen minima are typically around a few

hundred volts for common gases. Helium gas has the lowest Paschen minimum voltage. Most outgassing products have not had their Paschen curves measured. In the case of solar arrays, a coverglass that covers many cells must also make allowances for escape of outgassing products from adhesives. It must be treated for all intents and purposes as a vented enclosure (discussed below).

Fourth, the encapsulant must be able to withstand other aspects of the space environment for its design lifetime. Atomic oxygen, micrometeoroids and debris, and UV and X-ray exposure are some of the threats to the encapsulant. Glass stands up well to all of these environments. Some plastics do not.

D.2.3.1 Vented Enclosures

It should be pointed out that the use of a sealed pressure vessel eliminates environmental interactions, and this applies to plasma interactions as well. In the more general case, high-voltage systems other than solar arrays are usually contained in a vented enclosure. To avoid plasma interactions, care must be taken that plasma does not enter the enclosure and react with exposed conductors inside. The key requirement on such systems is that all openings must be smaller than the plasma Debye length, which depends on the plasma density and temperature. One can readily estimate the maximum opening consistent with such a requirement.

The plasma will be capable of maintaining electric fields over a distance of approximately one Debye length λ_D, which is given by

$$\lambda_D = (kTe/4\pi ne^2)1/2 = 7.43 \times 10^2 (Te/n)^{1/2} \text{ cm.} \qquad \text{(eqn. D.2.3.1)}$$

where Te is the electron temperature in eV, k is the Boltzmann constant, $\pi = 3.14159\ldots$, e is the charge of the electron, and n is the electron density in cm^{-3}. At a plasma density of $4x10^6$ cm^{-3}, one finds a minimum Debye length from 0.12 cm at 0.1 eV to 0.17 cm at 0.2 eV.

Openings in the experiment electronics enclosure must have smaller dimensions than this minimum to prohibit plasma interactions with the experiment electronics. Larger openings can be used if covered with an electrically connected conductive wire mesh of spacing less than the minimum Debye length. To provide a reasonable margin of safety, a general guideline is that no opening should exceed 0.10 cm in its largest dimension.

D.2.4 Arcing

D.2.4.1 On-Orbit Arc Detection

Usually in ground tests of solar arrays under simulated LEO plasma conditions, and especially when the array can undergo sustained arcing, an arc detection circuit is employed. It essentially looks for a rapid positive change of the array or arc site potential toward the plasma potential, since this must happen when electrons are emitted during an arc. For example, a coil can be placed around the solar array string output wire, and changes in the coil current will indicate a transient in the line. Conversely, one can sense the emission of copious electrons and use this for

arc detection. Further, the broadband EMI from an arc can be used for arc detection. On PASP-Plus, EMI detectors were used to determine when and where arcs occurred on-orbit. In any event, electrical detection techniques can unambiguously detect an arc when it occurs. Then, in ground tests, the power supply is electrically disconnected from the array to prevent the occurrence of sustained arcs that might damage or destroy the sample. Sometimes, the power supply is only disconnected when the arc continues for longer than 200 ms, for example, so that arcs that would be permanently sustained can be counted, but are not allowed to wreak their damage on the sample. Such arc detection and array protection circuits can be built and used on solar arrays operating on orbit. If this is done, rather than totally preventing arcs, the damage to the arc site is limited or prevented. In this way, the arcs that do occur become acceptable.

It must be obvious that the power to the LEO spacecraft will be interrupted whenever the array arc-circuit is broken. Rather than being the first line of defense against arcing, arc detection and array shunting must only be used when the disruptions they cause will be infrequent.

D.2.4.2 Prevention Techniques

The design of a solar array must consider the plasma environment and interactions with that environment. Arc prevention is extremely important. The following techniques have been shown in ground and flight tests to prevent arcs or minimize their damage:

a. If possible, use array string voltages of less than 55 V. No trigger arcs have been seen on LEO arrays of less than about 55 V string voltage or on anodized aluminum even under simulated micrometeoroid bombardment. Solar arrays coming out of eclipse will generate more voltage than when they operate at their max power point.

b. If solar array cell edges or interconnects are exposed to the LEO plasma and string voltages are greater than 55 V, the strings should be laid out on the substrate such that no two adjacent cells have a voltage difference of greater than 40 V. Sometimes a leapfrog arrangement will be sufficient. In other high-voltage arrays, the strings should be arranged parallel to each other. Serpentine strings can be used to prevent the array width from becoming prohibitive. If the string layout cannot be modified to prevent cells with more than 40 V difference being adjacent to each other (anything less than about 1 cm can be considered adjacent), then the total string voltage must be kept low enough that the initial (trigger) arcs do not take place. The lowest known array trigger arcing has occurred on thin-coverglass cells at about 75 V (PASP Plus results) (Soldi & Hastings, 1995).

c. For array string voltages greater than about 75 V, trigger arcs in LEO can be completely prevented by encapsulating the cell or array edges so they do not see the ambient plasma. The caveats mentioned above under “Encapsulation,” in appendix D, section D.2.3, must be followed. If encapsulation is not possible, a thorough array bakeout on orbit (1 week at 100° C or more) can get rid of contaminants and prevent trigger arcing up to about -300 V, or possibly more (see Vayner et al., 2002). Re-contamination can occur on “dirty” spacecraft (spacecraft with excessive venting, cold gas nozzles, etc.). Good encapsulation can prevent arcing up to 1000 V string voltage.

d. Sustained (or continuous) arcs can occur whenever trigger arcs occur and adjacent cells have more than 40 V potential differences. However, sustained arcs, in addition to this voltage threshold, have a current threshold below which they will not occur. It is believed that the current threshold is greater than about 0.5 amp. If the current produced by each cell is above this threshold, a single string can sustain arcs. If each cell is below this current threshold, then isolating separate strings of solar cells from each other will prevent other strings from "feeding" the arc site, and will prevent sustained arcs. This isolation can be achieved by using blocking diodes in each string. EOS-AM1, now called Terra, is an example (Snyder et al., 2000). Care must be taken that the power bus and/or other components do not have the conditions necessary for sustained arcing. On the Terra arrays, for instance, it was found that diodes used to block interstring currents did not prevent the bus power traces from having sustained arcing events. Covering all exposed bus conductors with Kapton® insulation finally solved the problem. Low-outgassing RTV can be used to cover bare conductors as well.

e. RTV grout between adjacent solar cells and strings that have a high voltage with respect to each other has been shown to effectively block sustained arcs between cells and strings. The degree of coverage, etc., is important in determining the final voltage threshold for sustained arcing.

f. Arrays of 300 V and greater string voltage must be fully encapsulated in order to prevent arcing. Caveats involved under "Encapsulation" in appendix D, section D.2.3, must be followed.

g. Finally, although design and construction are important in preventing trigger arcs and sustained arcs, each new solar array design implementation must be verified by testing in a simulated LEO plasma chamber before it can be sure not to arc. This is a critical step. The test bias voltage relative to the plasma should include the maximum array voltage when the arrays exit eclipse (or the highest floating potential expected on the spacecraft chassis). The interstring voltage should be at least as great as that expected anywhere on the solar arrays on orbit. A test should be conducted at the low temperatures experienced at eclipse exit.

APPENDIX E
MODELING

E.1 Spacecraft Charging

The severity and widespread nature of plasma interactions have led to a considerable investment in the development of computer models. Many empirical and semi-empirical models are available with varying levels of capability and fidelity. Since the physics of current collection is fully embodied in Poisson's equation, a first-principles treatment is both possible and practical. The most comprehensive such code that is available at this time for LEO is NASCAP/LEO (NASA Charging Analyzer Program/Low Earth Orbit). This code was developed as a follow-on to the original NASCAP computer program that dealt with spacecraft charging in geosynchronous orbit (Katz et al., 1981; Mandell et al., 1981; Rubin & Stevens, 1983).

A finite element-based solver, NASCAP/LEO, reasonably approximates the geometry of sophisticated satellites or subsystems. With an expandable materials database, it iteratively solves the potentials on all surfaces and electric fields in nearby space. The existing code was designed for mainframe and workstation deployment, makes many approximations necessitated by the limited desktop computing power of the mid-1980s, and has a reputation for having a steep learning curve. It is nevertheless credited with considerable success and, in the hands of a skilled user, is powerful and reliable.

A new version, currently being developed in conjunction with the U.S. Air Force, called NASCAP-2K, is now available. NASCAP-2K incorporates lessons learned over the past 18 years, takes full advantage of modern computing power with much more sophisticated algorithms, and is designed for easier use. Capable of modeling current collection and charging under LEO, GEO, and auroral conditions, NASCAP-2K should now supersede both NASCAP and NASCAP/LEO (Neergaard et al., 2001).

Of special interest here is a computer-modeling tool called EWB (Environmental WorkBench) (Chock & Ferguson, 1997). This tool, which can run on a desktop or laptop personal computer (PC), uses simple models of plasma environments and interactions to predict LEO spacecraft floating potentials, for example. Over 100 models of the LEO environment are included in this integrated code, and over 50 interactions models, including the plasma interactions models considered here. EWB was extensively funded by the ISS and is the official ISS plasma interactions tool. Detailed and extensive models of various ISS configurations are included with EWB, although the code can also be used to create and model a wide variety of different LEO spacecraft. Both EWB and NASCAP-2K are subject to International Traffic-in-Arms Regulations (ITAR) restrictions, and at present cannot be given to non-U.S. citizens. For more information on distribution of these codes, please see http://see.msfc.nasa.gov. European spacecraft charging modeling codes include the ESA Space Environment Information System (SPENVIS) family of codes, available on-line at http://www.spenvis.oma.be/spenvis/.

E.1.1 An Example

Figure 12 shows a plot with the result of an EWB calculation of potentials on the ISS mission build 12A. Here, a special model of ISS solar array current collection and ISS solar array mast wire current collection, based on PCU measurements of previous ISS mission builds, was constructed by Science Applications International Corporation (SAIC). The potentials shown were determined by iteration until the current balance equation was satisfied for ISS as a whole. In this figure, the PCUs were turned off to investigate charging under PCU failure conditions. It is clear that for this configuration, most of the vehicle charging is due to $\vec{v} \times \vec{B} \bullet \vec{l}$ effects across the long truss and solar array segments. Not shown are the EWB screens that detail the potentials and currents on each ISS component. EWB can also easily calculate the time dependence of all of the ISS potentials during an orbit and their dependencies on plasma parameters and changes in the detailed ISS configuration. Of course, EWB can also be used for other spacecraft. Figure 12 illustrates only how complex a system can be analyzed with this extremely useful computer code.

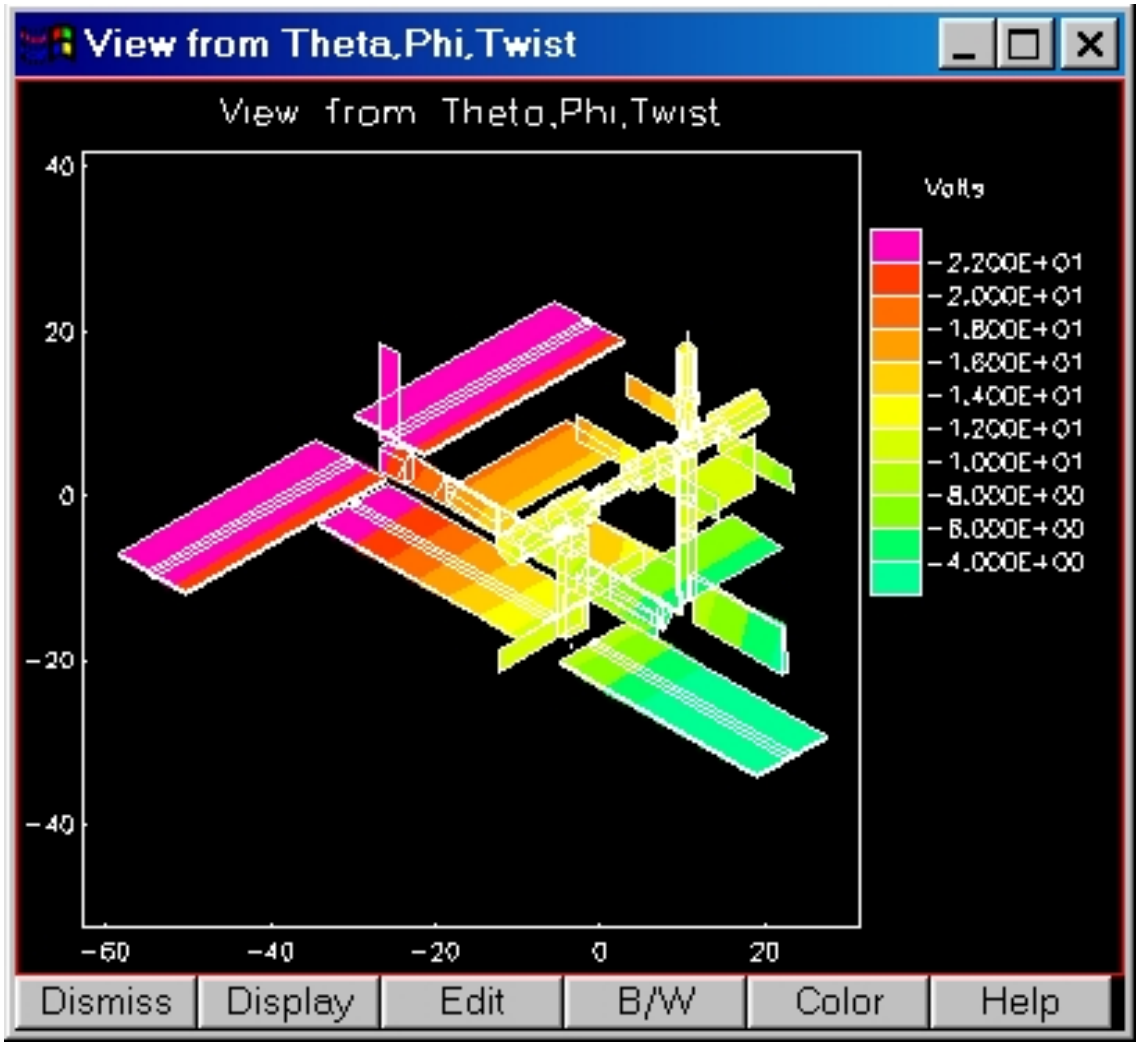

Figure 12— An EWB Contour Plot of ISS Potentials
(This is the 12A mission configuration at an arbitrary point in the orbit. The deviation from right-front to left-rear in the picture is due to $\vec{v} \times \vec{B} \bullet \vec{l}$ effects. In this picture, the velocity is toward the lower left, and the magnetic field is somewhat vertical. Taken from Ferguson and Hillard, 2003.)

E.1.2 Arcing

The process of electrical breakdown has not lent itself well to modeling, and solar arrays are no exception. The previously mentioned computer codes for determining potentials on all surfaces and electric fields in nearby space are certainly useful for solar arrays, but the actual initiation of an arc is extremely difficult to predict. Despite NASA's efforts to fund theoretical work in this area during the 1990s, no reliable model for arc initiation exists. Experience has shown that knowledge of the potential distribution is at best a rough indicator of the probability of an arc.

The complex geometries involved in cell construction and string layout along with the poorly understood properties of adhesives, coatings, and other materials often result in laboratory tests' behaving in unexpected ways. This emphasizes the need for testing of solar arrays in suitable space environmental chambers and ultimately as part of space experiments.

APPENDIX F
TESTING

The importance of testing in mitigating LEO spacecraft charging and its effects cannot be overestimated (Ferguson, 1996). A valid LEO arc test must take place in a vacuum of pressure less than about 250 microtorr. It must generate a plasma with an electron density of more than 10^5 electrons per cubic centimeter. The electron temperature should be less than about 3 eV but the lower the better, and the plasma should not be a streaming plasma (it should be essentially isotropic) unless special diagnostic techniques are used to determine the plasma properties. The sample temperature must be as low as the lowest sunlit temperature on orbit. To ensure that arcs will not occur in space, a sufficiently long waiting time must be used at each bias voltage that the arc rate is measured to be statistically significantly lower than the threshold arc rate. If the threshold is unknown, see Ferguson (1986) for a proper technique for establishing it in ground tests. Be aware that the arc rate at a given voltage usually decreases with time in the plasma; do not confuse this with an increasing arc voltage threshold (Ferguson, 1986). The chamber used for the tests should be big enough that the plasma sheath of the biased sample does not reach the chamber walls. Finally, use solar array design and building techniques that have been space qualified, whenever possible.

In LEO plasma testing, the array or anodized aluminum potential relative to the plasma (which in space is caused by spacecraft charging) is usually obtained by biasing the sample with a DC power supply. To investigate transient arcs, one must decouple the DC power supply from the arc current during an arc. This means the bias supply circuit must have a time constant greater than a few hundred microseconds, so the arc can build up and dissipate without being powered by the bias supply. This can be done by putting a large resistance in the arc circuit, and incorporating a capacitor to simulate the array or structure capacitance that would be discharged in the arc. For instance, if the on-orbit capacitance connected to the arc site is expected to be 0.1 microfarad, then this value capacitor can be used to provide current during the arc. With such a capacitor, the bias supply circuit can be given a 1-millisecond RC time constant (much greater than the arc time scale) with the use of a 10 kΩ series resistance. This effectively decouples the bias power supply from the arc. Of course, it also puts an upper limit on the arc rate attainable, because of recharge time considerations.

In non-destructive sustained arc testing, the series resistance should be adjusted to limit the maximum current to that expected in the arc, and a cutoff circuit should be employed to shut off the bias supply after a few hundred microseconds. Experience shows that an arc that continues under such circumstances for more than about 200 microseconds will be sustained. Arc current and/or voltage waveforms should be closely monitored to distinguish between transient and sustained arcs. Videotapes of arc locations are helpful for diagnostic purposes. If destructive sustained arcs are allowed to occur, the videotape can confirm the arc time duration.

Testing procedures used at the NASA GRC and MSFC plasma testing laboratories are summarized in Ferguson et al., 2005. For ESA and Japanese Space Agency (JAXA) testing techniques, see other papers in the same proceedings, session 2.

APPENDIX G
REFERENCES

Bonito, N.A.; Bounar, K.H.; McNeil, W.J.; Roth, C.J.; Tautz, M.F.; Vancour, R.P. (August 15, 1996). "Spacecraft Interactions Modeling and Post-Mission Data Analysis." Report Number RXR-96081. Bedford, MA, United States: Radex, Inc.
Brandhorst, H.; Best, S. (March 25, 2001). "Hypervelocity Impact Studies on Solar Cell Modules." Auburn University Report: AU-4-21839.
BSR/AIAA G-003B-2004 (2004). American National Standard, "Guide to Reference and Standard Atmosphere Models," American Institute of Aeronautics and Astronautics.
Button, R.; Brush, A.; Sundberg, R. (Jan 01, 1989). "Development and testing of a 20 kHz component test bed." IECEC-89. Proceedings of the Twenty-fourth Intersociety Energy Conversion Engineering Conference, Washington, D.C., August 6-11, 1989. New York: Institute of Electrical and Electronics Engineers. Vol. 1 (A90-38029 16-20), pp. 605-610.
Button, R.M.; Kascak, P.E.; Lebron-Velilla, R. (Feb 01, 2002). "Digital Control Technologies for Modular DC-DC Converters." NASA/TM-2002-211369.
Carruth, M.R., Jr.; Ferguson, D.C.; Suggs, R.; McCollum, M. (Jan 11, 2001). "ISS And Space Environment Interactions Without Operating Plasma Contactor." Paper presented at 39th Aerospace Sciences Meeting and Exhibit. (Jan 8-11, 2001). Reno, NV.
Chen, F.F. (1965). "Electric Probes," in *Plasma Diagnostic Techniques*, R.H. Huddlestone and S.L. Leonard, eds., Academic Press, New York, NY, pp. 113-200.
Cho, Mengu; Hastings, D.E. (Jan 01, 1991). "Dielectric charging processes and arcing rates of high voltage solar array." AIAA Paper #91-0605 presented at 29th Aerospace Sciences Meeting, Reno, NV, Jan 7-10, 1991.
Cho, M.; Hastings, D.E.; Kuninaka, H. (Jan 01, 1990). "Dielectric charging process in high voltage solar cell arcing." Paper presented at proceedings of 17th International Symposium on Space Technology and Science. Tokyo, Japan, May 20-25, 1990. Vol. 2 (A92-5345123-12). Tokyo, AGNE Publishing, Inc., 1990, pp. 1421-1426.
Chock, R.C. (1991a). "NASCAP/LEO Simulations of Shuttle Orbiter Charging During the SAMPIE Experiment." Paper presented at Fifth Annual Workshop on Space Operations, Applications, and Research (SOAR '91). Houston, Texas, July 9-11, NASA CP 3127, pp. 655.
Chock, R.C. (1991b). "NASCAP/LEO Simulations, SSF Solar Cell Geometries." Minutes of the Electrical Grounding Tiger Team Meeting, Boeing Trade Zone, Huntsville, Alabama, May 14-17.
Chock, R.; Ferguson, D.C. (1997). "Environments Workbench – An Official NASA Space Environments Tool." Paper presented at Proceedings of the 32nd Intersociety Energy Conversion Engineering Conference. Washington, D.C. IECEC 97452, pp. 753-757.
Cohen, H.A.; Cooke, D.L.; Evans, R.W.; Hastings, D.; Jongeward, G.; Laframboise, J.G.; Mahaffey, D.; Mcintyre, B.; Pfizer, K.A.; Purvis, C. (Oct 01, 1986). "Working group report on advanced high-voltage high-power and energy-storage space systems." *Space Technology Plasma Issues in 2001,* Jet Propulsion Laboratory.
"Computational procedure used in the development of the MSFC modified Jacchia model atmosphere." (1970). CE Environment criteria guidelines for use in space vehicle development, MSFC. SEE N70-40876 23-30.

Cooke, D.L.; Talbot, J.; Shaw, G. (Jan 31, 1994). "Pre-flight POLAR code predictions for the CHAWS space flight experiment." PL-TR-94-2056. Phillips Lab: Hanscom AFB, MA, United States.
Davis, V.A.; Katz, I.; Mandell, M.J.; Parks, D.E. (Sep 01, 1986). "Three dimensional simulation of the operation of a hollow cathode electron emitter on the Shuttle orbiter." Paper 16 presented at NASA, AIAA, and PSN, International Conference on Tethers in Space, Arlington, VA, Sept. 17-19, 1986.
Dunbar, W.G. (1988). Design Guide: Designing And Building High Voltage Power Supplies. Air Force Wright Aeronautical Laboratories: AFWAL-TR-88-4143, Vol. 2.
Ferguson, D.C. (Mar 01, 1985). "Ram-wake effects on plasma current collection of the PIX 2 Langmuir probe," *Spacecraft Environment Interactions Technology,* pp. 349-357.
Ferguson, D.C. (1996). "The Role of Space Plasma Simulation Chambers in Spacecraft Design and Testing." Thirty-first Intersociety Energy Conversion Engineering Conference Proceedings, Institute of Electrical and Electronics Engineers, pp. 2188-2192.
Ferguson, D.C. (Mar 01, 1986). The voltage threshold for arcing for solar cells in LEO: Flight and ground test results. NASA TM 87259.
Ferguson, D.C.; Gardner, B. (2002). "Modeling International Space Station (ISS) Floating Potentials." AIAA Paper #2002-0933 presented at 40th Aerospace Sciences Meeting and Exhibit, Reno, NV, Jan 14-17
Ferguson, D.C.; Hillard, G.B. (1997). "Lessons for Space Power System Design from the SAMPIE Flight Experiment." AIAA Paper #97-0087 presented at 35th Aerospace Sciences Meeting and Exhibit, Reno, NV, January 6-10.
Ferguson, D.C.; Hillard, G.B. (2003). Low Earth Orbit Spacecraft Charging Design Guidelines. NASA/TP—2003-212287.
Ferguson, D.C.; Hillard, G.B.; Snyder, D.B.; Grier, N.T. (1998). "The Inception of Snapover on Solar Arrays: A Visualization Technique." AIAA Paper #98-1045 presented at 36th Aerospace Sciences Meeting and Exhibit, Reno, NV, Jan 12-15.
Ferguson, D. C.; Hillard, G. B.; Vayner, B. V.; Galofaro, J. T. (2002). "High Voltage Space Solar Arrays." 53rd International Astronautical Congress of the International Astronautical Federation (IAF), Houston, TX, Oct. 10-19, 2002, IAC Paper 02-IAA.6.3.03
Ferguson, D.C.; Snyder, D.B.; Vayner, B.V.; Galofaro J.T. (1999). "Array arcing in orbit – From LEO to GEO." AIAA Paper #99-0218 presented at 37th Aerospace Sciences Meeting and Exhibit, Reno, NV, Jan. 11-14.
Ferguson, D. C.; Vayner, B. V.; Galofaro, J.T.; Hillard, G. B.; Vaughn, J.; Schneider, T. (2005). "NASA GRC and MSFC Space-Plasma Arc Testing Procedures." Proceedings of the 9th Spacecraft Charging Technology Conference, Tsukuba, Japan, April 4-8, 2005.
Galofaro, J.T.; Doreswamy, C.V.; Vayner, B.V.; Snyder, D.B.; Ferguson, D.C. (Apr 01, 1999). Electrical Breakdown of Anodized Structures in a Low Earth Orbital Environmental. NASA/TM-1999-209044.
Galofaro, J.; Vayner, B.; Degroot, W.; Ferguson, D. (Mar 01, 2002). The Role of Water Vapor and Dissociative Recombination Processes in Solar Array Arc Initiation. NASA TM 2002-211328.
Guidice, D.A.; Davis, V.A.; Curtis, H.B.; Ferguson, D.C.; Hastings, D.E. (Mar 01, 1997). "Photovoltaic Array Space Power Plus Diagnostics (PASP Plus) Experiment," Massachusetts Inst. of Tech. report. AD-A331959 PL-TR-97-1013.

Hastings, D.E. (1995). "A review of plasma interactions with spacecraft in low Earth orbit," *Journal of Geophysical Research*. Vol. 100, No. A8, pp. 14457-14483.
Hastings, D. E.; Cho, M.; Kuninaka, H. (Jan 01, 1992a). "The arcing rate for a High Voltage Solar Array – Theory, experiment and predictions," *Journal of Spacecraft and Rockets*. Vol. 29, Issue 4, pp. 538-554.
Hastings, D.E.; Cho, M.;, Kuninaka, H. (Jan 01, 1992b). "The arcing rate for a High Voltage Solar Array – Theory, experiment and predictions." AIAA Paper 92-0576 presented at the Aerospace Sciences Meeting and Exhibit, 30th, Reno, NV, Jan 6-9, 1992.
Hedin, A. (1987). "MSIS-86 thermospheric model." *Journal of Geophysical Research*. Vol. 92, pp. 4649-4660.
Hickey, M. (1988). The NASA Marshall engineering thermosphere model. NASA-CR-179359.
Hillard, G.B. (May 01, 1994). "Plasma chamber testing of advanced photovoltaic solar array coupons." *Journal of Spacecraft and Rockets*. Vol. 31, Issue 3, pp. 530-532.
Hillard, G.B.; Bailey, S.G.; and Ferguson, D.C. (2000). "Anodized Aluminum as Used for Exterior Spacecraft Dielectrics." Sixth Spacecraft Charging Technology Conference, AFRL-VS-TR-20001578, pp. 111-113.
Holm, R. (1999). *Electric Contacts: Theory and Applications*. Fourth edition, Springer Verlag.
Intersociety Energy Conversion Engineering Conference. Washington, D.C. IECEC 97452, pp. 753
Jongeward, G.A.; Katz, I.; Mandell, M.J.; Parks, D.E. (Dec 01, 1985). "The role of unneutralized surface ions in negative potential arcing." *IEEE Transactions on Nuclear Science.* Vol. NS-32, pp. 4087-409.
Katz, Ira, 2001. Spacecraft solar array charging control device. U.S. Patent #6,177,629.
Katz, I.; Cassidy, J.J.; Mandell, M.J.; Parks, D.E.; Schnuelle, G.W.; Stannard, P.R.; Steen, P.G. (Feb 01, 1981). "Additional application of the NASCAP code. Vol. 1: NASCAP extension." NASA-CR-165349.
Kennerud, K.L. (Mar 01, 1974). High voltage solar array experiments. NASA-CR-121280.
King, R.L. (1978). A computer version of the US Standard Atmosphere. NASA-CR-150778.
Koontz, S. (Feb. 22, 2005). "EVA Shock Hazard (ISS-EVA-312) Assessment and Control: 1) Strategy, Methods, and Forward Plan. 2) VIPER/PHALCON Role and Requirements," ISS VIPER Working Group.
Leung, P. (Nov 01, 1985). Characterization of EMI generated by the discharge of a VOLT solar array. NASA-CR-176537.
Malter, L. (1936). "Anomalous Secondary Electron Emission A New Phenomenon." *Phys. Rev*., Vol. 49, 478.
Mandell, M.J.; Katz, I.; Stannard, P.R. (Oct 01, 1981). Additional extensions to the NASCAP computer code, Vol. 1. NASA-CR-167855.
Metz, R.W. (1986). "Circuit Transients Due to Arcs on a High Voltage Solar Array." *Journal of Spacecraft and Rockets*, Vol. 23, Issue 5, pp. 499-504.
Miller, W.L. (Mar 01, 1985). "An investigation of arc discharging on negatively biased dielectric conductor samples in a plasma." *Spacecraft Environmental Interactions Technology*, pp.367-377 (SEE N85-22470 13-18).
Murphy, G.; Croley, D.; Ratliff, M.; Leung, P. (1992). "The Role of External Circuit Impedance in Dielectric Breakdown." AIAA Paper #92-0821 presented at 30th Aerospace Sciences Meeting and Exhibit, Reno, NV, January 6-9.

Murphy, G.; Pickett, J.; Dangelo, N.; Kurth, W.S. (Oct 01, 1986). "Measurements of plasma parameters in the vicinity of the Space Shuttle." *Planetary and Space Science.* Vol. 34, pp. 993-1004.
Neergaard, L.E.; Minow, J.; McCollum, M.; Cooke, D.; Katz, I.; Mandell, M.; Davis, V.; Hilton, J. (Jan 12, 2001). "Comparison of the NASCAP/GEO, POLAR, SEE Charging Handbook, and NASCAP-2K.1 Spacecraft Charging Codes." In the proceedings of the 7th Spacecraft Charging Technology Conference Noordwijk, April 23-27, 2001.
Parks, D.E.; Jongeward, G.A.; Katz, I.; Davis, V.A. (Jan 01, 1986). "Threshold determining mechanisms for discharges in high voltage solar arrays." AIAA Paper #86-0364 presented at AIAA, 24th Aerospace Sciences Meeting, Reno, NV, Jan 6-9, 1986.
Perez de la Cruz, C.; Hastings, D.E.; Ferguson, D.C.; Hillard, G.B. (May 01, 1996). "Data analysis and model comparison for solar array module plasma interactions experiment." *Journal of Spacecraft and Rockets.* Vol. 33, Issue 3, pp 438-446.
Prag, A.B. (1983). A comparison of the MSIS and Jacchia-70 models with measured atmospheric density data in the 120 to 200 km altitude range. NASA TR-0083 (3940-04)-1.
Purvis, C.K. (1985). "The Pix-II Experiment: An Overview," *Spacecraft Environmental Interactions Technology*, 1983, NASA CP-2359, AFGL-TR-85-0018, pp. 321-332.
Purvis, C.K.; Garrett, H.B.; Whittlesey, A.C.; Stevens, N.J. (1984). Design Guidelines for Assessing and Controlling Spacecraft Charging Effects. NASA TP-02361.
Raitt, W.J.; Siskind, D.E.; Banks, P.M.; Williamson, R.R. (Apr 01, 1984). "Measurements of the thermal plasma environment of the Space Shuttle." *Planetary and Space Science.* Vol. 32, pp. 457-467.
Reed, B.J.; Harden, D.E.; Ferguson, D.C.; Snyder, D.B. (2001). "Boeing's High Voltage Solar Tile Test Results." Seventeenth Space Photovoltaic Research and Technology Conference, Ohio Aerospace Institute, September 11-13.
Rubin, A.G.; Stevens, N.J. (Jan 25, 1983). "High voltage solar array models and Shuttle tile charging." AFGL Proc. of the AFGL Workshop on Nat. Charging of Large Space Struct. in Near Earth Polar Orbit, pp. 333-336.
Samir, U.; Stone, N.H.; Wright, K.H. (Jan 01, 1986). "On plasma disturbances caused by the motion of the Space Shuttle and small satellites – A comparison of in situ observations." *Journal of Geophysical Research.* Vol. 91, pp. 277-285.
Sargent, Noel B. (2002). Private communication. (NASA GRC))
Schneider, T.A., Carruth, M.R., Jr., Finckenor, M.M., Vaughn, J.A., Heard, J., and Ferguson, D. (2002). "An Experimental Investigation of the Effects of Charging on the International Space Station," Proceedings of the 7th Spacecraft Charging Technology Conference, Noordwijk, Netherlands, April 23-27, 2001.
Snyder, D.B. (Jan 01, 1984). Characteristics of arc currents on a negatively biased solar cell array in a plasma. NASA-TM-83728.
Snyder, D.B.; Ferguson, D.C.; Vayner, B.V.; Galofaro, J.T. (2000). "New Spacecraft-Charging Solar Array Failure Mechanism." Sixth Spacecraft Charging Technology Conference, AFRL-VS-TR-20001578, pp. 297-301.
Snyder, D.B.; Tyree, E. (Jan 01, 1984). The effect of plasma on solar cell array arc characteristics. NASA-TM-86887.

Snyder, D.B.; Vayner, B.V.; Ferguson, D.C. (1998). Private communication. (NASA GRC)
Soldi, James D.; Hastings, D.E. (Sept 01, 1995). "Arc Rate Simulation and Flight Data Analysis for the PASP Plus Experiment." MIT report AD-A301837, PL-TR-95-2126.
Stone, Nobie H.; Raitt, W.J. (Jan 01, 1998). The TSS-1R Electrodynamic Tether Experiment: Scientific and Technological Results. NASA Technical Report, NASA, Marshall Space Center.
Stone, Nobie H.; Wright, K.H.; Winningham, J.D.; Papadapolous, K.; Zhang, T.X.; Hwang, K.S.; Wu, S.T.; Samir, U. (Jan 01, 1998). "A Review of Scientific and Technological Results from the TSS-1R Mission." Paper presented at the Tether Technology Interchange Meeting, NASA, Marshall Space Flight Center.
Szalai, K.J.; Bonifazi, C.; Joyce, P.M.; Schwinghamer, R.J.; White, R.D.; Bowersox, K.; Schneider, W.C.; Stadler, J.H.; Whittle, D.W. (May 03, 1996). TSS-1R Mission Failure Investigation Board. NASA-TM-112426.
Upschulte, B.L.; Marinelli, W.J.; Carleton, K.L.; Weyl, G.; Aifer, E.; Hastings, D.E. (May 01, 1994). "Arcing of negatively biased solar cells in a plasma environment." *Journal of Spacecraft and Rockets.* Vol. 31, Issue 3, pp. 493-501.
"U.S. standard atmosphere." (1976) NOAA. NOAA-S/T-76-1562.
Vaughn, J.A., "Plasma Interactions with a Negative Biased Electrodynamic Tether," 8th Spacecraft Charging Technology Conference, Huntsville, AL, October, 2003.
Vaughn, J.A.; McCollum, M.B.; Kamenetzky, R.R. (May 01, 1997). "TSS-1R Failure Mode Evaluation." Thirty-first Aerospace Mechanisms Symposium, NASA Marshall Space Flight Center, pp. 309-320.
Vaughn, J.A. et. al. (2004). "Review of ProSEDS Electrodyanmic Tether Development," AIAA 2004-3507, 41st Joint Propulsion Conference, Fort Lauderdale, FL, July 12th-14th, 2004.
Vayner, B.V.; Doreswamy, C.V.; Ferguson, D.C.; Galofaro, J.T.; Snyder, D.B. (1998). "Arcing on Aluminum Anodized Plates Immersed in Low Density Plasmas," *Journal of Spacecraft and Rockets*, 35, 6, p. 805
Vayner, B.; Galofaro, J.; Ferguson, D. (Jul 01, 2001). Arc Inception Mechanism on a Solar Array Immersed in a Low-Density Plasma. NASA/TM-2001-211070.
Vayner, B.V.; Galofaro, J.T.; and Ferguson, D.C. "Interactions of High-Voltage Solar Arrays with Their Plasma Environment: Ground Tests," Journal of Spacecraft and Rockets, vol.41 no.6 (1042-1050), 2004.
Vayner, B.; Galofaro, J.; Ferguson, D.; Degroot, W. (2002). Electrostatic Discharge Inception on a High-Voltage Solar Array. NASA/TM-2002-211329.
Vayner, B.; Galofaro, J.; Ferguson, D.; deGroot, W.; Thomson, C.; Dennison, J.R.; Davies, R. (Nov 01, 1999). The Conductor-Dielectric Junctions In a Low Density Plasma. NASA/TM-1999-209408.

-